



Basic Aspects of Bone Mineralization

5

Paul Roschger, Barbara M. Misof,
and Klaus Klaushofer

Key Points

- The regular mineralization of the bone matrix seems not only to require the proper composition and structure of the organic matrix together with the presence of sufficient calcium (Ca) and phosphate but also cellular activity for mineral transport, deposition, and removal of mineralization inhibitors.
- Mineralization of the bone matrix occurs in two phases of different time scales, which are a fast primary and a slower secondary phase reflecting the nucleation and growth of the mineral particles in length, width, and thickness.
- Due to the ongoing activity of the bone cells and the time course of mineralization of newly formed bone matrix, bone is a spatially and temporarily heterogeneous material revealing a specific pattern of mineralization which is also an important determinant of bone material stiffness/elasticity.

- Deviations in the mineralization pattern due to alterations in bone turnover and/or mineralization kinetics measured in the bone biopsy sample from the patient provide important information for the clinician about underlying pathophysiology, interpretation of densitometry data, treatment decision and monitoring as well as fracture risk assessment.

Processes of Bone Mineralization

The majority of the presented results of bone mineralization and its distribution in this book chapter will have its focus on lamellar bone, which is formed by the concerted action of osteoblasts and deposited on a preexisting bone surface, which can be either freshly resorbed (remodeling) or resting (modeling). Four of such surfaces can be distinguished: trabecular, intracortical (osteonal), periosteal, and endosteal bone surfaces. There is some evidence that the mineralization processes might be somewhat different at these surfaces, as there are important differences in either cell activities or in mineral transport distances at these bone sites [1]. Noteworthy, differences of mineral and matrix properties between periosteal and intracortical surfaces in humeri of macaques were found recently by Raman microspectroscopy [2].

P. Roschger · B. M. Misof (✉) · K. Klaushofer
1st Medical Department Hanusch Hospital,
Ludwig Boltzmann Institute of Osteology at the
Hanusch Hospital of WGKK and AUVA Trauma
Centre Meidling, Vienna, Austria
e-mail: paul.roschger@osteologie.lbg.ac.at;
barbara.misof@osteologie.lbg.ac.at

In all these cases, mineralization is associated with a clear mineralization front extending to the entire surface of a forming bone packet or osteon up to a length of several hundred microns. This transition zone between nonmineralized matrix and the area where mineral accumulation takes place can be visualized by fluorescence labeling techniques.

However, mineralization processes as occur, for example, in *de novo* bone formation such as in membranous and endochondral ossification might be different. Nonetheless, as many of the observations of the first events in mineralization were made, in particular, in embryonic/fetal bone from animals, we also address these results from nonlamellar bone.

Early Events of Mineralization: Mineral Nucleation

The prerequisite of bone matrix mineralization is a microenvironment of a highly supersaturated solution of calcium and phosphate ions (Pi) of a proper ratio enabling the spontaneous nucleation and following growth of bone mineral hydroxyapatite (HA) crystals. Thus, the systemic as well as the local Ca⁺⁺ and phosphate ion (Pi) homeostasis is of crucial importance of adequate bone matrix mineralization.

Furthermore, the proper composition and organization of the organic bone matrix is important for its regular mineralization. Collagen type I is the main component of the organic matrix. It is a helical polypeptide which consists of two identical alpha 1 chains and one alpha 2 chain. This collagen matrix is formed by the osteoblasts and has to undergo a variety of intracellular and extracellular modifications before and after it is released from the osteoblast to form fibrils and fibers. In particular, investigation of the pathogenesis in brittle bone disease osteogenesis imperfecta has contributed to the understanding of the importance of these intra- and extracellular processes, including the formation of the collagen alpha-helices, their proper folding to triple-helices, the formation of fibrils, and later mineralization [3–6]. After collagen is released

from the osteoblasts, the collagen molecules form fibrils of a quasicrystalline structure in a self-assembling process with the collagen molecules arranged in a staggered pattern such that there is a 35 nm gap between the termini of collinear molecules [7, 8]. This staggering results in a pattern of alternating gap and overlap zones in the collagen molecules causing the electron contrast differences in transmission electron microscopy (TEM) images, which are visible by light and dark bands in the images [9, 10].

Before mineralization starts, the newly formed matrix (osteoid) seems to require some modifications known as the osteoid maturation, which lasts about 15 days in a healthy individual [11]. It is assumed that during this time, the organic matrix is transformed to provide a scaffold or framework for mineral deposition by the formation of collagen cross-links. Moreover, specific collagen residues were identified which might be suited to act as nucleation centers and might play an important role in onset and progression of mineralization [12]. However, collagen alone is not sufficient to drive organized mineralization; rather, specific non-collagenous proteins are needed which might act as nucleators. Candidates for these are proteins from the SIBLING (small integrin-binding ligand, N-linked glycoprotein) family, including matrix extracellular phosphoglycoprotein, osteopontin, dentin matrix protein 1, and bone sialoprotein. These proteins were reported to attract the mineral and to control growth; however, the same molecules might also inhibit mineralization [13, 14]. The presence and activity of alkaline phosphatase, which transfers pyrophosphate (PP) to phosphate ions (Pi) was found to be crucial for mineralization [15]. Depending on the ratio of PP/Pi, PP can act as initiator or inhibitor of mineralization [16, 17]. In a patient with hypophosphatasia (HPP) and chronic kidney disease-mineral and bone disorder (CKD-MBD), for instance, osteomalacia, together with high levels of pyrophosphate, was observed at the bone surface [18]. This suggests that pyrophosphate is blocking the onset of mineralization [18].

It is still not fully understood how the large amounts of mineral (or its components) are transported to the mineralization front, where they

need to be quickly disposable. However, there is strong evidence that, apart from the properties of the organic matrix, the bone cells play a direct role in regulation of the mineralization process [19, 20]. It is known that the osteoblasts' differentiation to osteocytes is intimately linked to the mineralization process [20, 21]. Cryo-TEM studies revealed matrix vesicles containing calcium-phosphate particles in blood vessels and in large amounts close to the forming bone surface in growing bone from an animal model [22]. This suggests that bone-derived exosomes (i.e., matrix vesicles) might not only transport a variety of different cell proteins to the extracellular matrix [23] but might also be a carrier for mineral. Such a transport mechanism would have the advantage to prevent any ectopic mineral precipitation in other tissues (e.g., blood vessels) and to carry the mineral to the place in bone where it is actually needed [22]. Matrix vesicles have been discovered already in the 1960s in connection with the mineralization of cartilage [24]. It is assumed that these matrix vesicles are released from cells, which have taken up large amounts of calcium and phosphate ions in their mitochondria. Calcium- and phosphorus-containing mineral aggregates were found in mouse osteoblast mitochondria [25]. Others showed that the intracellular mineral granules consist of disordered calcium phosphate, which is metastable and might serve as a potential precursor of carbonated hydroxyapatite [26]. Thus, the formation of mineral crystals seems to start already within the cells in the endosomes, which are subsequently released from the cell in exosomes [27]. However, it is still unknown how the vesicles are broken up and how their mineral content is transferred to the collagen. Furthermore, it has not been shown yet that this transport mechanism also plays a role in the mineralization of the lamellar structured osteoid in human bone.

The nature of the initial mineral deposits in the mineralization process is still under debate, while that of mature bone is relatively well known as a type of carbonated hydroxyapatite. Mineralization takes place in hydrated collagen, thus, the local degree of water content might play also an important role. Transient densification

stages of mineral were observed, such as a “dense liquid” phase and prenucleation clusters that form within it [28]. Transient precursors including amorphous calcium phosphate or octacalcium phosphate have been discussed for the initiation of biological apatite while others suggest that bone mineral is initiated via a very small, poorly crystalline, highly substituted hydroxyapatite (HA) mineral [29]. Both, either the existence of transient precursors [30] or the increase in apatite crystal size and crystallinity [31], might explain the differences between newly formed and mature bone apatite including chemistry, size, and solubility [29].

There is an ongoing discussion about where the mineral depositions occur within the bone matrix. As the striations of the collagen overlap-gap pattern can be also seen in mineralized tissues [9, 32, 33], it is assumed that the mineral is associated with this pattern. Using results from the mineralizing tendon, it was supposed that mineralization starts within the gap zones and the majority of mineral is located there [34, 35]. It is believed that adjacent gaps of the collagen are in contact with each other forming extended grooves which are filled by mineral [36]. During ongoing mineralization, the mineral particles might also grow beyond this space, form a continuous cross-fibrillar phase [37], and are also found associated with the fibrillar surface [38]. However, the distribution of mineral between intra- and extra-fibrillar spaces is somewhat controversial. While intra-fibrillar mineral might represent the bigger part and extra-fibrillar mineral the smaller portion of the overall mineral [39], an alternative model has also been discussed where most of the mineral is located in so-called “mineral lamellae” which are mineral-plates between adjacent collagen fibrils [40]. In any case, mineral in the inter-fibrillar space was suggested to be mechanically important as a component of “the glue” forming the connection between the mineralized collagen fibrils [41].

Generally, the mineral crystals (or particles) can be visualized individually by TEM [37, 42], atomic force microscopy (AFM) [43], or can be characterized as an average of several thousand to millions crystals by scattering techniques [44].

Scanning small-angle X-ray scattering (SAXS) together with scanning wide-angle X-ray scattering (WAXS) allows us to measure the length, the thickness, as well as the orientation of mineral particles [44]. In human bone, these types of measurements revealed mineral particle dimensions of approximately 15–200 nm with a thickness of 2–7 nm [45–47]. Furthermore, these studies have shown that the mineral particles are oriented by the collagen fibrils with the long axis of the platelets parallel to the long axis of the collagen fibril [48–50].

The Increase in Mineral Content: The Fast Primary and the Slow Secondary Phases

Once mineralization has started in the osteoid, the mineralization front proceeds with a certain speed toward the osteoid surface (termed mineral apposition rate (MAR) in histomorphometry) while osteoblasts still deposit new bone matrix. MAR is about 0.6 mm per day in cancellous bone and a somewhat higher in cortical bone [51, 52]. In addition to this spatial propagation of mineral in the bone matrix, mineral accumulation takes place with time within each mineralizing volume element of bone. This increase in mineral content thereby occurs with changing mineralization rates resulting in a specific time course of mineralization (“mineralization kinetics”). Likely the latter is not a natural constant, but it might vary with different conditions such as health or disease, skeletal site, individual’s age etc. [53–56].

Until now, it is not possible to follow the accumulation of mineral directly in a specific bone volume in humans as this would require repeated *in vivo* measurements in the identical bone volume element. However, attempts to measure the mineralization kinetics in small animals (mice) were done recently based on micro-computed tomography (μ CT) imaging [57, 58]. As the mineralization front in the osteoid is moving with a certain speed, it is possible to obtain indirectly the time course of mineralization by using techniques allowing to measure the mineral content

of bone volume elements in a spatially resolved manner with increasing distances (i.e., with increasing tissue age) from the mineralization front in bone samples. A first rapid increase (primary mineralization) and a subsequent slowdown of increase (secondary mineralization) in mineral content up to a final plateau level have been observed by analyzing line profiles of mineralization perpendicular to the mineralization front (Fig. 5.1) [59–64]. Such a biphasic behavior of mineralization rates might be explained by the following hypothetical scenarios: From a physical/chemical viewpoint, during the primary fast mineralization phase, the nucleation and the growth in predominantly two dimensions of the mineral particles may occur as well as single mineral clusters may be formed, which are subsequently fusing together. In the secondary slow mineralization phase, mineral particles are growing mainly in thickness and fusing more completely together. From the viewpoint of bone cells activity, the primary mineralization might occur essentially by the action of the osteoblasts which produce the matrix vesicles for supplying rapidly the mineral components in this initial phase of mineralization, while in the secondary phase, the mineral components might be transported by the osteocytic lacunar-canalicular network [65].

In principle, the secondary mineralization process leads to a positive correlation between mineralized bone tissue age and mineral content. Thus, apart from the cement lines (which differ in their organic matrix from the other bone tissue and are generally highly mineralized [66, 67]), the highest mineral content is generally found in the oldest tissue which is interstitial bone as a remnant from bone remodeling. However, also in osteonal cortical bone, more highly mineralized areas can be observed in the center of the osteon (adjacent to the Haversian canals) compared to that in its periphery [32, 68, and own observation]. This observation might either be due to a passive deposition of calcium and phosphate ions near to the Haversian canal or it might also indicate the presence of a tertiary mineralization process at least in cortical bone. This

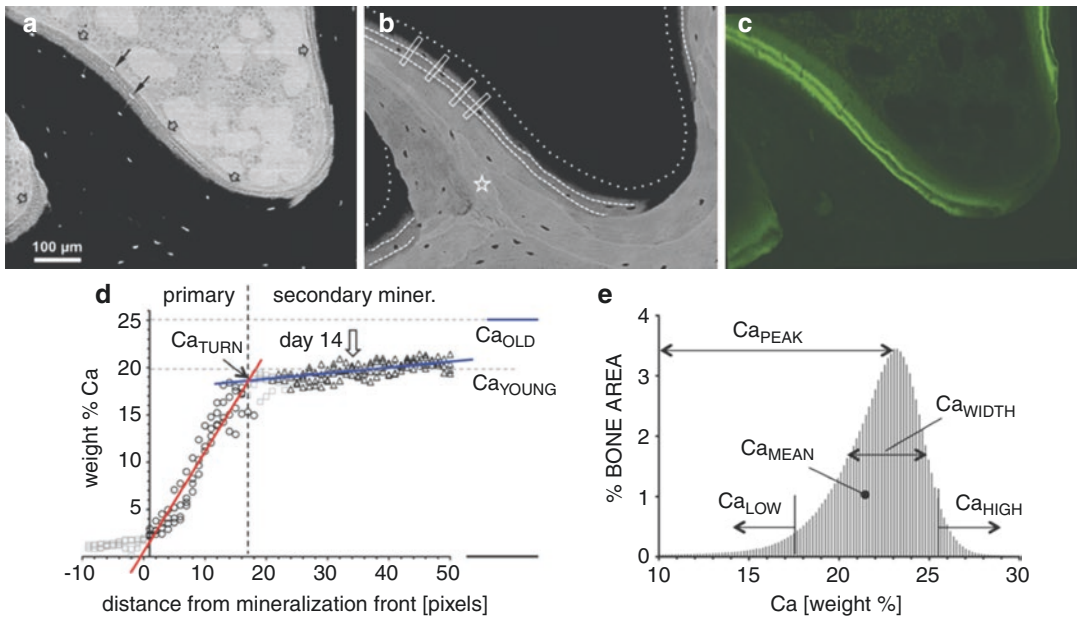


Fig. 5.1 A bone-forming site of trabecular bone— – scanning electron microscopic images acquired with a pixel resolution of $0.57\ \mu\text{m}$. **(a)** Backscatter electron image with special contrast setting showing all the mineralized matrix in black (not distinguishing between different mineral content) while the differences in grey level reveal the soft non-mineralized tissue embedded in PMMA (bone marrow). Black empty arrows point to lamellar osteoid, whereas black solid arrows point to pre-osteocytes (osteoid osteocytes). **(b)** The same site shown by the backscatter electron image with a calibrated contrast setting for quantitative backscatter electron imaging (qBED) [63]. The grey levels are correlated with the local mineral content (the brighter the higher the mineral content). Bone packets of different gray levels can be seen within the trabecular feature. The newly forming ones at the surface have the lowest gray levels. White star indicates old interstitial bone. Dotted lines are indicating the borderline of the osteoid as seen in **(a)**. Dashed lines are indicating the position of the fluorescence bands of tetracycline double labeling of the moving mineralization front (dynamic indices of bone formation) as obtained from **(c)**. The white bars, perpendicular through the mineralization front, indicate the regions where mineralization line profiles were analyzed as shown in **(d)**. **(c)** Corresponding confocal laser scanning microscope image from the identical block surface as in **(a)** and **(b)**: Parallel running fluorescent double labels are visualized. In this case, the distance between the labels corresponds to 12 days and the position of the second label (latter time point) corresponds to 6.5 days before biopsy. **(d)** Mineralization line profiles pooled from the four regions indicated in **(b)** (bars); X-axis at zero position indicates the onset of mineralization (i.e., the mineralizing front).

Red, regression line from data with circle symbols showing the fast primary mineralization phase (steep slope). Blue, regression line from data with triangle symbols showing the slow secondary mineralization phase (flat slope); gray square symbols indicate the data not included in the regression analysis. The intersection point of both regression lines defines the calcium concentration at the transition from primary to secondary mineralization (Ca_{TURN} , 18.5 wt % Ca). The empty arrow indicates the position in the center of the two fluorescent labels and corresponds to a tissue age of 14 days. Note, the labelled areas are already in the secondary phase and their corresponding Ca-content mirrors the level of early secondary mineralization named Ca_{YOUNG} , (at 20 wt % Ca.) in contrast the level of the oldest bone reflects the interstitial bone (star in **(b)**) named Ca_{OLD} (at 25 weight % Ca). Consequently, the secondary mineralization varies from 20 to 25 wt % Ca corresponding to its tissue age. **(e)** Bone mineralization density distribution (BMDD) deduced from image **(B)**. The five derived BMDD parameters are indicated: Ca_{MEAN} , the average degree of mineralization, obtained from the integrated area of the BMDD curve; Ca_{PEAK} , the position of the peak indicating the most frequently (typical) calcium concentration within the sample; Ca_{WIDTH} , the width at half maximum of the BMDD, a parameter for the heterogeneity of mineralization. Ca_{LOW} , the percentage of areas with low (below 17.68 weight %) mineralization reflecting areas undergoing primary mineralization; Ca_{HIGH} , the percentage of areas with high (beyond 25.30 weight %) mineralization. These cut-off levels were established using the normative cancellous BMDD (see Fig. 5.2), and correspond to the 5th and 95th percentiles of calcium concentrations.

additional mineral seems to be added later to the level reached by secondary mineralization. There is some evidence that this phenomenon is associated with the higher density of osteocytic canaliculi found in the central area of the osteons [69, 70].

It is widely accepted that the mineral accumulation in the organic bone matrix is accompanied by the replacement of the free water present in the matrix [71]. For instance, this is confirmed by vibrational spectroscopy studies on plastic (polymethylmethacrylate, PMMA) embedded bone samples showing a clear decrease in the PMMA vibrational peak in tissue areas of increasing mineral content/tissue age [72, 73]. Since during the embedding process PMMA substitutes for the water in the sample, the PMMA peak is representing indirectly the water content and mirrors, therefore, also the nanoporosity of the bone material. According to experimental data on lateral spacing of the collagen molecules (1.1 nm in dry, 1.55 nm in wet, and 1.25 nm in mineralized bone conditions) in combination with theoretical model considerations, the collagen fibril could theoretically take up to a maximum of 56 vol% (volume percent) mineral corresponding to 30 wt% (weight percent) Ca until all the free water is replaced [74, 71]. However, in human bone, a maximum mineral content of only around 25 to 27 wt% Ca is found [75], which is consistent with the aforementioned 1.25 nm collagen spacing found for bone. Interestingly, this means that in reality, the mineralization seems to be limited by additional mechanisms and not only by the available space within the fibrils and moreover that water is still present in fully mineralized bone (in particular collagen-bound water [76, 77]). There is evidence that the number of nucleation centers for the mineral crystals and their growth to final size might be the determinant of the final level of mineral achieved in bone [78, 79]. An example where this was demonstrated is bone in osteogenesis imperfecta. In this disease, an increased degree of mineralization compared to healthy bone was observed [80–82]. First, this was linked to the higher amount of water present in the defective collagen which could be replaced by mineral during mineralization processes [81].

However, the degree of mineralization was increased independent of whether the patients had structurally aberrant collagen (qualitative mutation) due to the underlying collagen mutation or only a reduced quantity of structurally normal collagen (quantitative mutation) [55]. This points rather toward a scenario, where the number of nucleation centers might be a crucial determinant of the final bone mineral content [80]. Indeed, the results from X-ray scattering experiments gave evidence for normal-sized crystals in osteogenesis imperfecta suggesting that the higher bone matrix mineralization is achieved by more densely packed mineral particles [79]. In this context, it should be mentioned that the bone material has not to be considered as a nanocomposite material of two components (collagen and mineral), but rather than as a three-component system including water. Recent studies emphasized the tremendous role of the hydration status of the bone material on its mechanical performance [76, 77, 83, 84]. The more dehydrated the material is, the stiffer and less ductile are its properties. In the case of osteogenesis imperfecta, the increased mineral content as well as the reduced hydration of the collagen would explain the extreme brittleness of the material. It can be assumed that the level of about 25 wt% Ca in normal healthy bone resulting also in a certain residual hydration of the matrix might provide optimal stiffness and ductility.

Mineralization Distribution in Bone

The matrix mineralization pattern as seen in images such as Fig. 5.1b and the resulting mineralization distribution of bone can be considered as a kind of fingerprint of bone at the material level [85]. It reflects the history of bone cell activity, like conditions of low and high bone turnover rates as well as changes/abnormalities in the mineralization kinetics [86]. When visualizing bone material, for instance, in the backscatter electron mode of the scanning electron microscope, areas (so-called bone packets) with different gray levels can be seen (Fig. 5.1). These bone packets or bone structural

units (BSUs) were formed by osteoblasts during one bone formation cycle. Given the mineralization processes as described above, the mineral content of bone is dependent on its tissue age. Recently formed BSUs have lower degree of mineralization than older ones. Consequently, the mineralization distribution depends strongly on the bone formation/turnover situation. If bone formation is high, many BSUs are formed; thus, a high percentage of the bone packets will have young tissue age and correspondingly low mineral content. This is the reason why growing bone from children has on average a lower degree of mineralization compared to bone from adult individuals [78, 87]. Additionally, in the case of high bone resorption, there is low chance that a bone packet will become old and will have accordingly high mineral content as the probability for resorption is high. Thus, in high bone turnover (high formation and resorption), the overall bone tissue age is low. Vice versa, when bone turnover is low, the tissue age will be high, and thus a larger percentage of higher mineralized bone packets will be present [63, 88]. This pattern of mineralization can be described/quantified by deduction of gray-level (Ca content) histograms from the microscopic images the so-called bone mineralization density distribution (BMDD) (Fig. 5.1). For the measurement of the BMDD, spatially resolved techniques are necessary. Several methods with spatial resolution from few microns to submicron resolution, which make use of different physical mechanisms, are available for this purpose (see in the following).

Before an overview of methods for the measurement of the local mineral content and its variation in bone at the material level is given, the difference of the latter to the clinically (in vivo) measured bone mineral density (BMD) at the organ level by dual X-ray absorptiometry has to be mentioned. BMD is widely used as a surrogate measure of bone strength and is determined by the amount/volume of bone present and its material density (the latter is dominated by the calcium content). Hence, low BMD might be due to low bone volume or due to decreased bone mineral content or due to a combination of both. It is

important to have this in mind when interpreting BMD data, in particular, for the evaluation of treatment effects [89].

Measurement of the Mineralization Distribution

One important technique, which measures the mineral content of bone in a spatially resolved manner, is vibrational spectroscopy (infrared and Raman microspectroscopies). It makes use of the absorption or inelastic scattering of light (infrared light or laser light of different wavelength from infrared to ultraviolet, respectively) by the bone sample [90–93]. The chemical groups of the bone sample are not stationary but undergo twisting, bending, rotation, and vibration causing absorption or inelastic scattering at specific wavelengths, which are characteristic for structure and environment of the molecules. Most commonly, the spectra are analyzed by measuring a specific absorption peak height, peak areas, peak width, and calculation of the ratios of specific peak areas (e.g., mineral to matrix ratio). The strength of these spectroscopic techniques is that both basic components mineral and organic matrix can be analyzed, however, it usually can provide only relative amounts between these components.

Other methods utilize the attenuation of an X-ray beam by the sample. The oldest method is microradiography which measures the X-ray absorption in an about 100- μm -thick bone sections [94, 95] using either photographic films or in newer systems a digital detector [96]. The resulting gray levels on the film or the measured intensities on the detector reflect the X-ray intensities transmitted through the bone slice and are evaluated by microdensitometric methods. The most modern technique is synchrotron radiation micro computed tomography (SR- μCT). It measures the X-ray absorption under different angles in similar concept as in computer tomography scanners in the clinic, however in contrast to the latter SR- μCT analyzes the gray levels for information on the bone mineralization [97, 98]. More modern techniques additionally combine the

information from X-ray tomography with phase retrieval (“holotomography”) which enhances the sensitivity of mineral content measurement [99].

A further frequently applied method is quantitative backscatter electron imaging (qBEI or qBSE) which measures the intensity of the backscattered electron signal from the surface of a block bone sample [63, 100–102]. In bone, this signal is correlated to the local calcium content, which enables the calcium mapping of a sectioned bone area.

In all methods, the result is a frequency histogram of pixels (or voxels) with different calcium concentrations occurring in the sample, the so-called bone mineralization density distribution (BMDD) derived from the acquired images (Fig. 5.1) [63]. Typically, the BMDD is normalized to the measured bone area (i.e., the area under the frequency histogram is 100%). The typical BMDD is similar to a bell-shaped curve, however, shows some asymmetry with higher portion of low than highly mineralized areas. In order to perform statistical analysis between different BMDDs, special parameters deduced from the BMDD were successfully introduced describing the mean, the most frequently occurring and the variation in Ca content. Furthermore, the percentage of bone area with very low or high mineral contents is quantified (Fig. 5.1).

The measurement of the BMDD requires bone samples. For scientific purposes, these can be different types of postmortem bone samples. However, commonly these are transiliac bone biopsy samples, which were primarily obtained for histopathologic examinations for the differential diagnosis or classification of bone diseases or as part of clinical trials to analyze treatment effects. The additional histologic/histomorphometric characterization of the biopsy is an enormous advantage as it enables to interpret the BMDD data in combination with histomorphometric data. In addition, these analyses can be combined (at defined anatomical locations) with other techniques (such as Raman spectroscopy, scattering techniques, ultrasound microscopy, nanoindentation, etc.) to get detailed information on structure/function relationship of the bone material.

Bone Mineralization Distribution in Healthy Individuals

Trabecular bone was found to have a relatively low biological variation from early adulthood up to 100 years of age. The authors’ own reference BMDD (based on qBEI measurements) revealed a mean calcium concentration of 22.3 ± 0.45 weight % Ca (mean \pm standard deviation) measured in healthy individuals (Fig. 5.2) [103]. Comparison of the average degree of mineralization in humans showed neither significant differences between skeletal sites (iliac crest, vertebrae, patella, femoral neck, or head), nor dependency on other biological factors such as sex and ethnicity. While small increases of average calcium concentration of cancellous bone with age were observed recently [104], other studies did not find such an increase with age [95, 103]. In any case, the merely small variation of the mineralization distribution of cancellous bone in healthy adult individuals (within an age range of about 25–100 years) made it possible to establish normative data which are the basis for comparison to bone mineralization in pathologi-

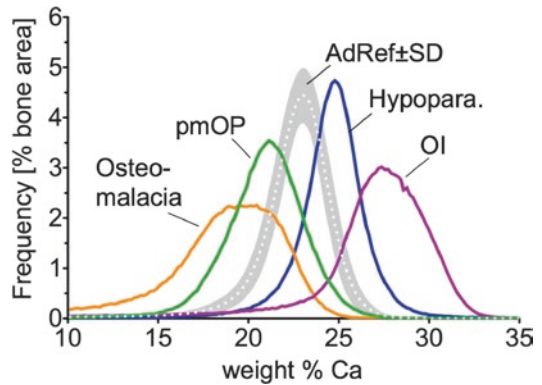


Fig. 5.2 BMDD in health and in examples of diseased bone: *AdRef* adult healthy reference of cancellous bone—white dotted line represents the mean of each histogram bin value and the gray band its standard deviation from a cohort of 52 individuals [103], *osteomalacia* due to coeliac disease, *pmOP* postmenopausal osteoporosis (high bone turnover) [128], *Hypopara.* hypoparathyroidism post surgery [133], *OI* osteogenesis imperfecta in an adult patient due to mutation in the gene region responsible for the C-terminal propeptide cleavage site of procollagen [147].

cal cases and after treatment (Fig. 5.2). Remarkably, despite these general small variations in healthy cancellous bone, the close relationship between bone turnover/formation and bone mineralization could still be detected. For example, in a cohort of healthy premenopausal women, the average degree of mineralization was negatively correlated with bone turnover (albeit within the normal range) and positively correlated with heterogeneity of bone matrix mineralization [105].

Normative BMDD data could also be established in transiliac bone biopsy samples from children aged 1.5–20 years [87]. This is extremely helpful in detecting and describing rare diseases, which are associated with a bone phenotype [106–108, 79]. For the cancellous and cortical compartment, a mean and standard deviation of 20.95 ± 0.57 and 20.31 ± 0.93 wt % Ca, respectively, were found. This level of bone mineralization is distinctly lower and its inter-individual variation is higher compared to adults, which can be explained by the higher bone formation rate and growth spurts in developing iliac crest of children.

All together the relatively constant mineralization around 22 weight % Ca is likely indicating the existence of an ideal range in degree and heterogeneity of bone matrix mineralization in relation with the trabecular bone's biological function and mechanical performance. Deviations in both directions, to lower and to higher mineralization densities, were reported to be associated with bone fragility [109]. Similar, heterogeneity of mineralization (and other properties such as lamellar orientation) has a consequence for the mechanical properties. Neither too little nor too much might be favorable as heterogeneity might hinder crack propagation while it might also facilitate crack initiation [110, 111].

Cortical compact osteonal bone, however, was found to show generally a higher average mineral content compared to cancellous bone. Additionally, differences in cortical bone mineralization itself also exist generally throughout the human skeleton [112]. However, it is remarkable that to date, systematic studies on cortical bone mineralization are rather sparse, although

cortical bone represents about 80% of the entire skeleton, and is thus considered most relevant for weight bearing and also bone fragility. Skull bone (e.g., mandibles) seems to be generally more highly mineralized as the femoral midshaft or the cortex of the iliac crest [113]. Thus, intraindividual differences between cortical compartments and between cortical and trabecular compartments of the skeleton seem to exist. As explained above, the mineralization distribution of bone is closely related to both the bone turnover rate and the mineralization kinetics. It is intuitively clear that bone volumes within the thick cortex might have less probability to be remodeled compared to those in the relatively thinner trabecular struts which are closer to the surface where bone resorption takes place. Thus, cortical bone is expected to have higher tissue age, because of reduced bone turnover rates, which is reflected by in average higher degree of mineralization. Indeed, this was found for bone at the femoral neck and midshaft compared to cancellous bone [112, 114, 75]. On the other hand, it was observed that bone mineralization is clearly related to loading demands in the femoral neck, which might be accomplished by an adaption of the mineralization kinetics. Bone mineral content was found higher at the inferior compared to the superior region, which is predominantly loaded in compression, while the superior region is loaded in tension [114, 115]. Furthermore, the differences between cortical mineralization at femoral midshaft bone and cancellous bone might not be fully explained by the differences in bone turnover between these sites [56, 116]. This suggests that additionally to the variation in bone turnover, differences in mineralization kinetics among different skeletal sites and between cortical and trabecular bone might also exist due to the loading demands. Noteworthy, about 25% higher mineral/matrix ratios in human ossicles compared to femoral bone were reported albeit, it has to be mentioned that ossicles are not only comprised of lamellar bone but also woven bone and mineralized cartilage [117]. This high mineral content, however, can be considered as an adaptation to their function of sound transmission [117].

It is remarkable that the two cortical plates of transiliac bone biopsy samples were found to be very similar in mineralization with that of the corresponding cancellous bone compartment [118]. Moreover, the degree of mineralization of cortical bone was strongly correlated with that of trabecular bone. Individuals with relatively higher cancellous bone mineralization also have higher cortical bone mineralization and vice versa, which suggests a tight coupling of bone turnover in these two compartments of the iliac crest. For this reason, one should be cautious to extrapolate the BMDD findings in the iliac crest to other cortical sites. In this context, it would be helpful to establish normative BMDD reference values for different fracture relevant skeletal sites in relationship to iliac cortical bone for fracture risk prediction.

Mineralization Distribution in Diseased Bone

The aforementioned link between bone turnover and the mineralization kinetics with the bone mineralization distribution suggest that alterations in the former processes have an impact on the latter mineralization distribution. In specific diseases, the bone mineralization distribution clearly follows the deviation in bone turnover from normal, that is, high turnover is associated with low tissue age and low mineralization densities and vice versa. In other cases, however, an altered time course and/or final level of mineral accumulation within each bone packet occurs.

Postmenopausal osteoporosis (pmOP) with high fracture risk (“fracture disease”) is one of the chronic diseases, which has been affecting a high portion of the elderly population with increasing incidence during the last decades [119]. To facilitate noninvasive diagnosis and assessment of fracture risk, osteoporosis is commonly diagnosed by low BMD according to the WHO classification. However, in a large portion of the patients, bone fragility is not attributable to reduced BMD. Thus, changes in bone material quality, specifically bone matrix mineralization, might affect the mechanical competence of bone.

There seems to exist some variety in bone turnover abnormalities in pmOP [120–122]; however, usually women with pmOP are diagnosed with high turnover [123, 124]. High turnover, in particular, during perimenopause and the first years after decline of estrogens, together with the imbalance of bone formation and resorption is leading to gradual bone loss, and this alters the bone mineralization distribution in pmOP by decreasing the average degree and increasing the heterogeneity of bone matrix mineralization compared to healthy individuals (Fig. 5.2) [125–131].

In addition to these findings in pmOP, a close relationship of the bone mineralization distribution with bone turnover was observed also in other pathologic conditions. For instance, patients with hyperparathyroidism reveal high bone turnover and correspondingly low bone mineralization densities [95, 132]. Vice versa, patients with hypoparathyroidism have suppressed bone turnover and increased matrix mineralization (Fig. 5.2) [133]. Low bone turnover and increased bone matrix mineralization were also reported for children with inflammatory bowel disease [134], for children after organ transplantation [135], and for young patients with chronic kidney disease and growth retardation [136], which were all associated with reduced bone formation and turnover. Deviations from normal bone mineral content and distribution were also described in association with increased bone fragility in several investigations [114, 115, 137–139].

In contrast to the aforementioned examples, where the bone mineralization distribution follows the deviation in bone turnover from normal, there exist also pathological conditions where the change of bone turnover is not predictive for the mineralization distribution. Male patients with osteoporosis and premenopausal women with idiopathic osteoporosis, for instance, were observed to have low bone turnover but also a low degree of bone mineralization [105, 140–142]. These unexpected findings might indicate that either the mineralization processes are slower or the final level of mineralization is reduced in these patients. Such modified material properties per se might be caused by altered osteoblast function in

idiopathic forms of osteoporosis associated with differences in the organic matrix and the mineralization kinetics thereof [141, 105]. The latter was also suggested for patients carrying COL1A1 Sp1 polymorphisms with increased bone fragility and reduced and more heterogeneous matrix mineralization [143].

Osteogenesis imperfecta is another example where the mineralization distribution does not follow the aforementioned correlation with bone turnover [80]. Many forms of this genetic disease have been described so far, including those with mutations in the collagen genes (“classical forms”) and those more recently discovered having mutations in genes encoding for proteins which are associated with extracellular modification, cleavage of terminal endings, etc. While almost all of these forms are reported with high turnover [144], they have also in common an elevated mineral content of bone which contributes to bone brittleness [80, 145]. However, the hypermineralized bone matrix might occur in parallel with hyperostoidosis in new forms of osteogenesis imperfecta [146–148]. This indicates that the onset of mineralization in the osteoid is delayed, but once mineralization has begun, it goes up to higher levels than normal (Fig. 5.2).

Another group of patients are those whose calcium and/or phosphate homeostasis is highly disturbed due to calcium ions uptake deficiency, kidney disease (with impaired renal phosphate excretion), and/or phosphate wasting. Both Ca and phosphate deficiency lead to mineralization defects with highly mineralized bone matrix coexisting with only weakly mineralized and nonmineralized bone matrix (Fig. 5.2). Such mineralization defects might occur in cases of renal osteodystrophy in patients with chronic kidney disease (CKD-MBD) [136], as well as in fibroblast growth factor 23 (FGF23)-induced hypophosphatemia as, for example, in patients with X-linked hypophosphatemic rickets (XLH) [149] or tumor-induced osteomalacia [54]. In a child with XLH, the transiliac biopsy sample showed areas of unmineralized bone within the mineralized bone matrix giving bone a mottled appearance [149]. Also, the mineralized bone matrix showed differences in the

BMDD, revealing an increased frequency of bone areas with low calcium concentrations (i.e., low material density) in the patient’s biopsy sample. Furthermore, bone mineralization abnormalities due to disturbance of calcium and phosphate metabolism might occur in celiac disease [63]. Just recently a patient with Crohn’s disease and severe hypophosphatemic osteomalacia linked to iron substitution has been described (Fig. 5.2) [150].

Hypophosphatasia (HPP) which is caused by mutations in genes encoding for the tissue non-specific alkaline phosphatase enzyme (TNSALP) is also an example where bone mineralization is disturbed [15, 151]. Clinically HPP is essentially identified by low serum alkaline phosphatase levels and increased levels of alkaline phosphatase substrates (pyrophosphate and pyridoxal-5’-phosphate). The deficiency of TNSALP activity leads to extracellular accumulation of its natural substrates including pyrophosphate which is a potent inhibitor of mineralization. The common radiographic finding in children with HPP is poorly mineralized bone [151, 152]. However, a huge range of severity in the phenotype has been described from lethal forms without mineralization of the skeleton to adults who are virtually asymptomatic [153, 154]. In general, the phenotypic severity present is related to the severity of the inherited TNSALP mutation. Bone biopsy samples from adult patients revealed (depending on the severity of HPP) the presence of osteomalacia and changes in the bone mineralization distribution [155].

Interestingly, there is strong evidence that bone matrix which has been nonmineralized for longer time in the aforementioned cases might be able to mineralize, if treatment is able to establish the proper Ca and Phosphate levels in the patient [18, 150]. The most impressive example are the children with HPP, who develop normally mineralized bone after alkaline phosphatase enzyme replacement therapy (asfotase alfa) which enables the mineralization of already formed bone matrix [152, 156]. So far, information on the mineralization changes at material level due to enzyme replacement treatment was obtained in mouse models, where increases in tissue mineral density

were reported with treatment [157, 158]. Apart from enzyme replacement treatment, an interesting observation was made in sequential biopsy samples from one adult patient with HPP (Fig. 5.3) [18]. In the first biopsy obtained from this patient, large unmineralized or poorly mineralized areas which showed diffuse fluorescence labeling were visible. In the later biopsy samples, this diffuse labeling was embedded in mineralized bone tissue, further indicating that osteoid, which does not mineralize for longer periods,

might also be mineralized as soon as an appropriate environment exists and inhibitors of mineralization are removed from the matrix [18]. In this context, the case of iron treatment-induced osteomalacia in a patient with Crohn's disease should be mentioned as well [150]. The intravenous iron therapy induced a hypophosphatemia, which led to a severe osteomalacia as detected in the transiliac bone sample and contributed to a progressive decline of BMD (DXA). Cessation of iron therapy and the supplementation with phosphate

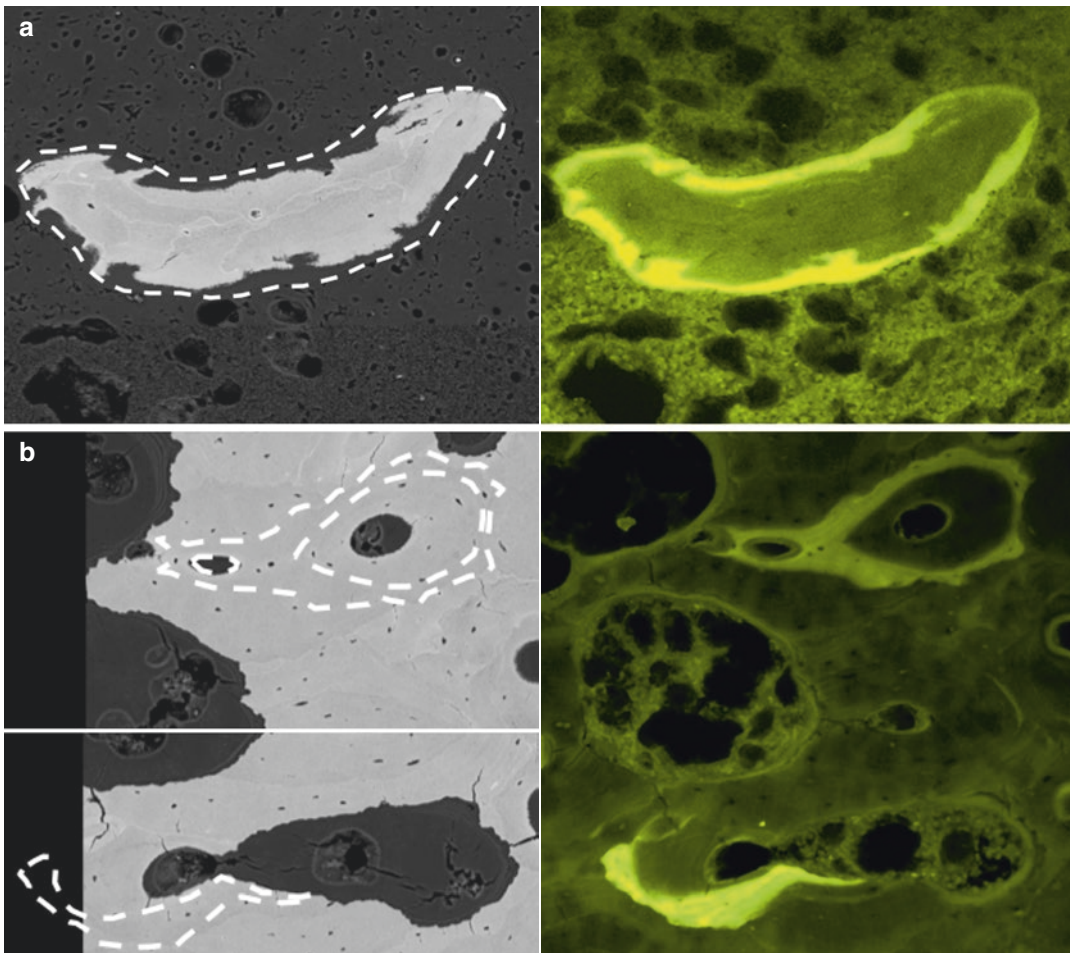


Fig. 5.3 Mineralization of aged osteoid in sequential biopsy samples from a patient with hypophosphatasia and renal failure [18]: (a) (left): backscatter electron (BE) image of a trabecular feature of the first transiliac biopsy sample with history of alendronate treatment and tetracycline labeling prior to biopsy: dashed white line indicates the border of the osteoid seam, which is visualized by confocal laser scanning microscopy (CLSM) of identical

sample surface in a (right) as bright diffuse fluorescent region. (b) pair of BE (left) and CLSM (right) image of the second biopsy after stopping alendronate treatment (second biopsy without tetracycline labeling before). Diffuse labelled regions are now mineralized and embedded in mineralized bone tissue formed later as indicated by the dashed lines in BE.

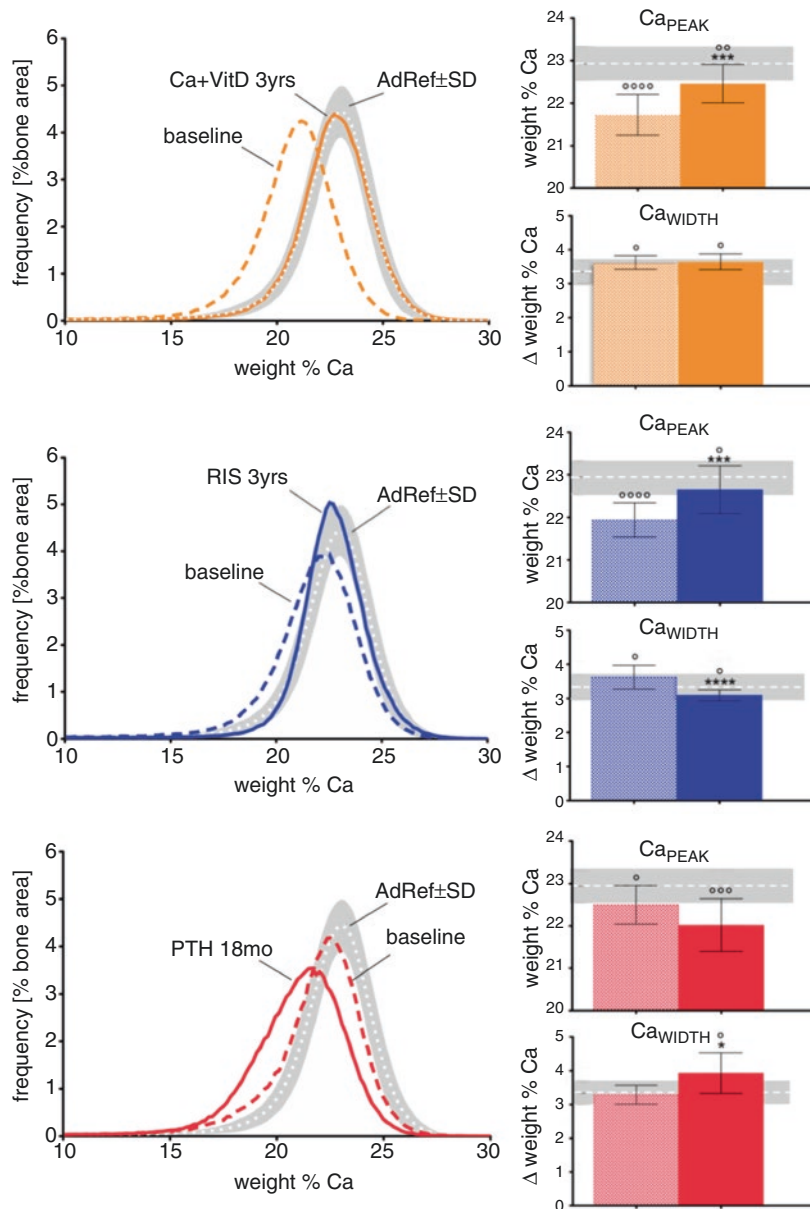
was associated with a prompt positive response in BMD, which was likely due to filling of the osteoid matrix with mineral.

The examples mentioned above showed that information about the status of bone turnover in the individual is important for the correct interpretation of bone mineralization distribution. When increases in bone turnover rates are not associated with low bone mineral content and vice versa, alterations in the mineralization kinetics have to be taken into consideration.

Bone Mineralization Distribution after Treatment of Osteoporosis

Treatment of osteoporosis aims to decelerate bone loss and/or to increase bone volume. The different mechanisms of action of anabolic or antiresorptive agents (see Chaps. 12 and 14) are reflected in the typical changes in the distribution of bone mineralization accompanying the different types of treatment (Fig. 5.4) [159]. Noteworthy, during therapy, bone turnover/formation undergoes rapid

Fig. 5.4 The typical changes in BMDD of pmOP after treatment with calcium and vitamin D, RIS (risedronate) or PTH. Left column: examples of individual BMDD curves of paired biopsy samples before and after treatment. Right column: statistical analysis of BMDD-parameters Ca_{PEAK} and Ca_{WIDTH} of experimental groups before and after treatment [64, 128]. Bars indicate group mean values; error bars show standard deviations. Gray horizontal band indicates healthy adult reference data of cancellous bone (mean \pm SD) [103]. The left bars show baseline values, and the right bars values after treatment.



changes as shown by the significant changes in the biochemical bone markers. For instance, a sudden drop of the C-telopeptide of type I collagen (CTX) and the intact procollagen I N-propeptide (PINP) within as early as 1 week to few weeks depending on the type of bisphosphonate (BPs) was reported [160]. This rapid change pushes bone turnover and also the mineralization distribution out of an equilibrium stage making an observation of transient effects on the mineralization distribution possible [161] as will be described for antiresorptive treatment.

Treatment with Calcium and Vitamin D

Commonly, patients participating in a clinical trial receive calcium and vitamin D supplementation already before starting the active antiosteoporosis (or the placebo) treatment. However, the study design of the Vertebral Efficacy with Risedronate Therapy, North American trial (VERT-NA) and the Multiple Outcomes of Raloxifene Evaluation trial (MORE) provided an insight into the calcium and vitamin D effects in paired biopsy samples. Comparison of the bone matrix mineralization outcomes before and after treatment with calcium and vitamin D (and placebo) showed a shift to higher mineralization densities due to treatment [127, 128, 162]. The comparison of bone mineralization from the patients from the VERT-NA trial reference data revealed that these patients had undermineralized bone matrix at baseline [128]. This suggests that calcium and vitamin D deficiency alone is likely a cause of undermineralization, which can be offset by calcium and vitamin D supplementation (Fig. 5.4).

Hormone Replacement Therapy

Treatment with estrogen or with selective estrogen receptor modulators (SERMs) provide skeletal benefits in postmenopausal osteoporosis where estrogen deficiency is an important contributor to the pathogenesis of osteoporosis [163]. In studies

where bone matrix mineralization was analyzed in postmenopausal osteoporotic patients after treatment with estrogen or SERMs, an increase in degree of mineralization or mineral:matrix ratio was reported [162, 164, 165].

Antiresorptive Treatment

Bisphosphonates (BPs) have been used for treatment of osteoporosis for several decades [166]. BPs inhibit bone resorption as they get adsorbed to mineral surfaces in bone, where they interfere with the action of the bone-resorbing osteoclasts. Their antiresorptive action is rather fast as already mentioned while the changes in mineralization are much slower (given the time of several months required for completion of one remodeling cycle [167]). Due to the sudden drop in bone resorption and formation in relation to the time which is needed for achieving a new bone turnover equilibrium, the measured effects of antiresorptive therapy on the bone mineralization distribution depend on the duration of therapy, short term (up to about 3 years) versus long term (5 years and longer). For short-term BP therapy (including alendronate, risedronate, ibandronate and zoledronic acid), a significant decrease in the heterogeneity of mineralization has been reported [130]. Moreover, the percentage of low mineralized areas is decreased and the average degree of mineralization is increased [130]. Noteworthy, these changes occur in osteoporotic bone which has generally lower degree and increased heterogeneity of mineralization than healthy bone before therapy. Moreover, part of these BP effects, in particular the reduction in mineralization heterogeneity, seem to be transient. After longer therapy duration, the heterogeneity together with the degree of bone mineralization is normalized (Fig. 5.4) [128, 168]. In the context of long-term antiresorptive treatment, it has to be noted that while no adverse effect on the bone mineralization distribution per se could be observed, the increasing occurrence of atypical femoral fractures have been reported [169]. These are therefore unlikely related to the changes in mineralization during therapy but more likely

related to the suppression of the internal fracture-repair mechanism by the decreased osteoclast activity (see also Chap. 21).

The BP effect on bone turnover and its consequences on bone matrix mineralization are well understood [63, 88, 98, 126, 128–130, 159, 161, 170–173]; however, it is unclear whether the change in turnover is also accompanied (at least to some extent) by a change in mineralization kinetics. Studies on bone from treated animals suggested no significant effect of alendronate or risedronate on the temporal course of mineral accumulation in bone [174]. However, on the other hand, it is assumed that the BP which is absorbed to the mineral might alter the chemistry and electrostatic properties of the bone surface which might be detected by osteoblasts [175]. Data from vibrational microspectroscopy suggested deviations in material properties from normal after different types of BP [176] as well as differences in the matrix formed under subsequent anabolic therapy in BP pretreated patients [177, 178].

While the effects of BP on human bone mineralization are well known as shown by the results from the numerous biopsy studies, much less is known about these effects in treatment with *denosumab*, a human monoclonal antibody to RANKL (see Chap. 15). Long-term safety and efficacy of this osteoporosis treatment have been published recently [179]; histologic evaluation of transiliac biopsy samples showed normal bone microarchitecture without evidence of adverse effects on mineralization or the formation of lamellar bone [180]. First data on bone mineralization in transiliac biopsy samples from patients were published recently [131]. In this study, bone biopsies from participants of the FREEDOM and FREEDOM extension study were analyzed. Outcomes showed an increase in the average degree and a decrease in the heterogeneity of mineralization in both cancellous and cortical compartments in denosumab versus placebo-treated patients.

There has been a debate whether therapy with *strontium ranelate* (SrR) exerts a combination of anabolic and concurrent antiresorptive action in bone [181]. Chavassieux and colleagues reported no evidence for anabolic but antiresorptive action only [182], which is in agreement with the

bone matrix mineralization outcomes based on qBEI in transiliac biopsy samples [183]. Similar to above-mentioned fluoride, the element strontium gets incorporated into the bone mineral crystal; in the young bone packets formed during SrR therapy, it replaces approximately 5 at% of calcium [183, 184]. It was shown also that the strontium content of the bone matrix increases with increasing bone volume formed under therapy [185]. In contrast to fluoride, strontium seems not to change the mechanical properties of the bone material [184]. As strontium is an element with high atomic number, its incorporation into mineral, however, influences the measurement of BMD (mimics higher bone mass in DXA), bone volume by computed tomography, as well as bone mineralization and makes the evaluation of the genuine effects of SrR challenging [183].

Anabolic Treatment

Anabolic treatment with *sodium fluoride* was considered for treatment of postmenopausal osteoporosis some decades ago. However, the treatment was not widely accepted as it was recognized that despite the large increases in bone volume, bone fragility was not decreased in the treated patients [186]. It was recognized that bone formed under treatment was altered and mechanically inferior to normal bone as the element fluoride gets incorporated into the mineral resulting in a disturbance of the normal collagen–mineral relationship [187]. Abnormally large mineral particles and abnormal size distributions of the mineral particles have been observed [188, 189] together with mineralization defects [190] and abnormally high degree of bone mineralization [63]. Due to these adverse effects, systemic sodium fluoride has not gained wide use, although attempts have been undertaken to decrease the adverse effects by sustained-release sodium fluoride given on an intermittent basis [191].

The current options of anabolic therapy are treatment with *parathyroid hormone* (PTH 1–84), *teriparatide* (PTH 1–34), or *abaloparatide*. Significant changes in the bone mineralization

distribution with PTH or teriparatide are commonly observed. In line with an increase in bone formation, decreases in the average degree and increases in the heterogeneity of bone mineralization were reported (Fig. 5.4) [64, 192]. The decrease in average mineralization density can be explained by the increase in the percentage of low mineralized bone areas, which is a typical change in the BMDD in a situation of high bone formation/turnover. The experimental findings were confirmed by computed modeling, which revealed the occurrence of a “shoulder” in the BMDD at lower calcium concentrations after 1 year anabolic treatment [161]. Interestingly, only 1 year with PTH 1–84 was sufficient to change the mineralization distribution significantly in patients with hypoparathyroidism, a condition with suppressed bone turnover at baseline [133]. Similarly, an increase in the portion of low mineralized bone was observed after sequential treatment with bisphosphonates followed by teriparatide in postmenopausal osteoporotic patients [193]. BMDD data from combined treatment with anabolic and concurrent antiresorptive treatment are lacking so far.

More recently, treatment with *parathyroid hormone-related peptide (PTHrP, abaloparatide)* has come into focus (see also Chaps. 14 and 15) [194]. In a recent study, histologic analysis revealed no evidence of adverse effects on mineralization in bone biopsy samples from treated patients [195]; however, no data on its effect on the mineralization distribution exist so far. Similar for alternative novel anabolic agents such as *sclerostin antibody* therapy (see Chap. 16), only bone mineralization data from animal models are available yet. For treated rats [196], as well as for a treated mouse model of osteogenesis imperfecta, no significant effects on mineralization were reported [197].

Summary

The proper mineralization of the bone matrix is important for its mechanical performance. In bone from healthy individuals, relatively small variation in the distribution of cancellous bone

mineralization could be observed which enabled to establish reference mineralization data that can be used for differential diagnosis. Indeed, deviations from normal have been observed in several bone diseases. Increased bone turnover associated with lowered average tissue age and lowered mineralization is found in postmenopausal osteoporosis. Antiosteoporosis therapies exert antiresorptive or anabolic mechanisms in the skeleton. Both treatment options have typical effects on the bone mineralization distribution. While antiresorptive therapy decreases bone resorption and formation resulting in higher tissue age, and thus a higher degree of mineralization, anabolic therapy increases the bone formation resulting in relatively young bone tissue having low mineralization densities. These changes might play a role in enhancing mechanical properties after treatment and have to be considered when evaluating the BMD changes in diseases and/or after treatment. In cases where predominately the Ca and Phosphate metabolism is disturbed, extreme deviations from normal BMDD can be observed showing shifts to lower calcium concentrations together with a strong increase in heterogeneity of mineralization.

Acknowledgments The authors gratefully thank Prof. Dr. Dr.h.c. Peter Fratzl (Max Planck Institute of Colloids and Interfaces, Department of Biomaterials, Potsdam, Germany) for the numerous studies in collaboration with the Ludwig Boltzmann Institute of Osteology during more than two decades which represent a significant contribution in this text. Moreover, they thank him for the discussion and his fruitful comments on this chapter.

References

1. Jones DB, Nolte H, Scholübbbers JG, Turner E, Veltel D. Biochemical signal transduction of mechanical strain in osteoblast-like cells. *Biomaterials*. 1991;12(2):101–10.
2. Paschalis EP, Gamsjaeger S, Hassler N, Klaushofer K, Burr D. Ovarian hormone depletion affects cortical bone quality differently on different skeletal envelopes. *Bone*. 2017;95:55–64. <https://doi.org/10.1016/j.bone.2016.10.029>. Epub 2016 Nov 4.
3. Prockop DJ. Osteogenesis imperfecta: phenotypic heterogeneity, protein suicide, short and long collagen. *Am J Hum Genet*. 1984;36(3):499–505. Review.

4. Forlino A, Cabral WA, Barnes AM, Marini JC. New perspectives on osteogenesis imperfecta. *Nat Rev Endocrinol.* 2011;7(9):540–57. <https://doi.org/10.1038/nrendo.2011.81>. Review.
5. Marini JC, Reich A, Smith SM. Osteogenesis imperfecta due to mutations in non-collagenous genes: lessons in the biology of bone formation. *Curr Opin Pediatr.* 2014;26(4):500–7. <https://doi.org/10.1097/MOP.0000000000000117>. Review.
6. Eyre DR, Weis MA. Bone collagen: new clues to its mineralization mechanism from recessive osteogenesis imperfecta. *Calcif Tissue Int.* 2013;93(4):338–47. <https://doi.org/10.1007/s00223-013-9723-9>. Review.
7. Hodge AJ, Petruska JA. Recent studies with the electron microscope on ordered aggregates of the tropocollagen molecule. In: Ramachandran, G.N., Ed., *Aspects of Protein Structure*, Academic Press, New York, Academic Press; 1963; 289–300.
8. Fratzl P, editor. *Collagen – structure and mechanics*. ISBN: 978-0-387-73905-2. Springer Science+Business Media, LLC; 2008. 504 pages.
9. Probst KS, Lees S. Visualization of crystal-matrix structure. In situ demineralization of mineralized Turkey leg tendon and bone. *Calcif Tissue Int.* 1996;59(6):474–9.
10. Starborg T, Kalson NS, Lu Y, Mironov A, Cootes TF, Holmes DF, Kadler KE. Using transmission electron microscopy and 3View to determine collagen fibril size and three-dimensional organization. *Nat Protoc.* 2013;8(7):1433–48. <https://doi.org/10.1038/nprot.2013.086>.
11. Eriksen EF, Gundersen HJ, Melsen F, et al. Reconstruction of the formative site in iliac trabecular bone in 20 normal individuals employing a kinetic model for matrix and mineral apposition. *Metab Bone Dis Relat Res.* 1984;5:243–52.
12. Landis WJ, Silver FH. Mineral deposition in the extracellular matrices of vertebrate tissues: identification of possible apatite nucleation sites on type I collagen. *Cells Tissues Organs.* 2009;189(1–4):20–4. <https://doi.org/10.1159/000151454>.
13. Gericke A, Qin C, Spevak L, Fujimoto Y, Butler WT, Sørensen ES, Boskey AL. Importance of phosphorylation for osteopontin regulation of biomineralization. *Calcif Tissue Int.* 2005;77(1):45–54.
14. George A, Veis A. Phosphorylated proteins and control over apatite nucleation, crystal growth, and inhibition. *Chem Rev.* 2008;108(11):4670–93. <https://doi.org/10.1021/cr0782729>.
15. Millán JL, Whyte MP. Alkaline phosphatase and hypophosphatasia. *Calcif Tissue Int.* 2016;98(4):398–416. <https://doi.org/10.1007/s00223-015-0079-1>. Review.
16. Millán JL. The role of phosphatases in the initiation of skeletal mineralization. *Calcif Tissue Int.* 2013;93(4):299–306. <https://doi.org/10.1007/s00223-012-9672-8>. Review.
17. Orriss IR, Arnett TR, Russell RG. Pyrophosphate: a key inhibitor of mineralisation. *Curr Opin Pharmacol.* 2016;28:57–68. <https://doi.org/10.1016/j.coph.2016.03.003>. Review.
18. Cundy T, Michigami T, Tachikawa K, Dray M, Collins JF, Paschalis EP, Gamsjaeger S, Roschger A, Fratzl-Zelman N, Roschger P, Klaushofer K. Reversible deterioration in hypophosphatasia caused by renal failure with bisphosphonate treatment. *J Bone Miner Res.* 2015;30(9):1726–37. <https://doi.org/10.1002/jbmr.2495>.
19. Murshed M, Harmey D, Millán JL, McKee MD, Karsenty G. Unique coexpression in osteoblasts of broadly expressed genes accounts for the spatial restriction of ECM mineralization to bone. *Genes Dev.* 2005;19(9):1093–104.
20. Atkins GJ, Findlay DM. Osteocyte regulation of bone mineral: a little give and take. *Osteoporos Int.* 2012;23(8):2067–79. Review.
21. Feng JQ, Ye L, Schiavi S. Do osteocytes contribute to phosphate homeostasis? *Curr Opin Nephrol Hypertens.* 2009;18(4):285–91. <https://doi.org/10.1097/MNH.0b013e32832c224f>. Review.
22. Kerschnitzki M, Akiva A, Shoham AB, Koifman N, Shimoni E, Rechav K, Arraf AA, Schultheiss TM, Talmon Y, Zelzer E, Weiner S, Addadi L. Transport of membrane-bound mineral particles in blood vessels during chicken embryonic bone development. *Bone.* 2016;83:65–72. <https://doi.org/10.1016/j.bone.2015.10.009>.
23. Pethő A, Chen Y, George A. Exosomes in extracellular matrix bone biology. *Curr Osteoporos Rep.* 2018;16(1):58–64. <https://doi.org/10.1007/s11914-018-0419-y>. Review.
24. Bonucci E. Fine structure of early cartilage calcification. *J Ultrastruct Res.* 1967;20:33–50.
25. Boonrungsiman S, Gentleman E, Carzaniga R, Evans ND, McComb DW, Porter AE, Stevens MM. The role of intracellular calcium phosphate in osteoblast-mediated bone apatite formation. *Proc Natl Acad Sci U S A.* 2012;109(35):14170–5. <https://doi.org/10.1073/pnas.1208916109>.
26. Mahamid J, Sharir A, Gur D, Zelzer E, Addadi L, Weiner S. Bone mineralization proceeds through intracellular calcium phosphate loaded vesicles: a cryo-electron microscopy study. *J Struct Biol.* 2011;174(3):527–35. <https://doi.org/10.1016/j.jsb.2011.03.014>.
27. Shapiro IM, Landis WJ, Risbud MV. Matrix vesicles: are they anchored exosomes? *Bone.* 2015;79:29–36. <https://doi.org/10.1016/j.bone.2015.05.013>. Review.
28. Dorvee JR, Veis A. Water in the formation of biogenic minerals: peeling away the hydration layers. *J Struct Biol.* 2013;183(2):278–303. <https://doi.org/10.1016/j.jsb.2013.06.007>.
29. Grynopas MD, Omelon S. Transient precursor strategy or very small biological apatite crystals? *Bone.* 2007;41(2):162–4.
30. Weiner S. Transient precursor strategy in mineral formation of bone. *Bone.* 2006;39(3):431–3.
31. Grynopas MD, Bonar LC, Glimcher MJ. Failure to detect an amorphous calcium-phosphate solid phase in bone mineral: a radial distribution function study. *Calcif Tissue Int.* 1984;36(3):291–301.

32. Engström A. Chapter 7 Aspects of the molecular structure of bone. In: Bourne GH. The biochemistry and physiology of bone. 2nd ed. Vol. 1 Structure. Academic Press; Elsevier Inc., 1972.
33. Quan BD, Sone ED. Structural changes in collagen fibrils across a mineralized interface revealed by cryo-TEM. *Bone*. 2015;77:42–9. <https://doi.org/10.1016/j.bone.2015.04.020>.
34. Traub W, Arad T, Weiner S. Origin of mineral crystal growth in collagen fibrils. *Matrix*. 1992;12(4):251–5.
35. Landis WJ, Song MJ, Leith A, McEwen L, McEwen BF. Mineral and organic matrix interaction in normally calcifying tendon visualized in three dimensions by high-voltage electron microscopic tomography and graphic image reconstruction. *J Struct Biol*. 1993;110:39–54.
36. Weiner S, Traub W. Organization of hydroxyapatite crystals within collagen fibrils. *FEBS Lett*. 1986;206(2):262–6.
37. Reznikov N, Bilton M, Lari L, Stevens MM, Kröger R. Fractal-like hierarchical organization of bone begins at the nanoscale. *Science*. 2018;360(6388). pii: eaao2189 <https://doi.org/10.1126/science.aao2189>.
38. Landis WJ, Hodgens KJ, Song MJ, Arena J, Kiyonaga S, Marko M, Owen C, McEwen BF. Mineralization of collagen occurs on fibril surfaces: evidence from conventional and high voltage electron microscopy and three-dimensional imaging. *J Struct Biol*. 1996;117:24–35.
39. Alexander B, Daulton TL, Genin GM, Lipner J, Pasteris JD, Wopenka B, Thomopoulos S. The nanometre-scale physiology of bone: steric modelling and scanning transmission electron microscopy of collagen-mineral structure. *J R Soc Interface*. 2012;9(73):1774–86. <https://doi.org/10.1098/rsif.2011.0880>.
40. Schwarcz HP. The ultrastructure of bone as revealed in electron microscopy of ion-milled sections. *Semin Cell Dev Biol*. 2015;46:44–50. <https://doi.org/10.1016/j.semcdb.2015.06.008>. Review.
41. Gupta HS, Seto J, Wagermaier W, Zaslansky P, Boesecke P, Fratzl P. Cooperative deformation of mineral and collagen in bone at the nanoscale. *Proc Natl Acad Sci U S A*. 2006;103(47):17741–6.
42. Arsenault AL, Grynblas MD. Crystals in calcified cartilage and cortical bone of the rat. *Calcif Tissue Int*. 1988;43:219–25.
43. Hassenkam T, Fantner GE, Cutroni JA, Waever JC, Morse DE, Hansma PK. High-resolution AFM imaging of intact and fractured trabecular bone. *Bone*. 2004;35:4–10.
44. Pabisch S, Wagermaier W, Zander T, Li C, Fratzl P. Imaging the nanostructure of bone and dentin through small- and wide-angle X-ray scattering. *Methods Enzymol*. 2013;532:391–413. <https://doi.org/10.1016/B978-0-12-416617-2.00018-7>. Review.
45. Fratzl P, Gupta HS, Paschalis EP, Roschger P. Structure and mechanical quality of the collagen-mineral nanocomposite in bone. *J Mater Chem*. 2004;14:2115–23.
46. Wess T, Alberts I, Hiller J, Drakopoulos M, Chamberlain AT, Collins M. Microfocus small angle X-ray scattering reveals structural features in archaeological bone samples: detection of changes in bone mineral habit and size. *Calcif Tissue Int*. 2002;70(2):103–10.
47. Kaspersen JD, Turunen MJ, Mathavan N, Lages S, Pedersen JS, Olsson U, Isaksson H. Small-angle X-ray scattering demonstrates similar nanostructure in cortical bone from young adult animals of different species. *Calcif Tissue Int*. 2016;99(1):76–87. <https://doi.org/10.1007/s00223-016-0120-z>.
48. Rinnerthaler S, Roschger P, Jakob HF, Nader A, Klaushofer K, Fratzl P. Scanning small angle X-ray scattering analysis of human bone sections. *Calcif Tissue Int*. 1999;64(5):422–9.
49. Zizak I, Roschger P, Paris O, Misof BM, Berzlanovich A, Bernstorff S, Amenitsch H, Klaushofer K, Fratzl P. Characteristics of mineral particles in the human bone/cartilage interface. *J Struct Biol*. 2003;141(3):208–17.
50. Granke M, Gourrier A, Rupin F, Raum K, Peyrin F, Burghammer M, Saïed A, Laugier P. Microfibril orientation dominates the microelastic properties of human bone tissue at the lamellar length scale. *PLoS One*. 2013;8(3):e58043. <https://doi.org/10.1371/journal.pone.0058043>.
51. Rehman MT, Hoyland JA, Denton J, Freemont AJ. Age related histomorphometric changes in bone in normal British men and women. *J Clin Pathol*. 1994;47(6):529–34.
52. Recker RR, Kimmel DB, Parfitt AM, Davies KM, Keshawaraz N, Hinders S. Static and tetracycline-based bone histomorphometric data from 34 normal postmenopausal females. *J Bone Miner Res*. 1988;3(2):133–44.
53. Paschalis EP, Fratzl P, Gamsjaeger S, Hassler N, Brozek W, Eriksen EF, Rauch F, Glorieux FH, Shane E, Dempster D, Cohen A, Recker R, Klaushofer K. Aging versus postmenopausal osteoporosis: bone composition and maturation kinetics at actively-forming trabecular surfaces of female subjects aged 1 to 84 years. *J Bone Miner Res*. 2016;31(2):347–57. <https://doi.org/10.1002/jbmr.2696>.
54. Nawrot-Wawrzyniak K, Varga F, Nader A, Roschger P, Sieghart S, Zwettler E, Roetzer KM, Lang S, Weinkamer R, Klaushofer K, Fratzl-Zelman N. Effects of tumor-induced osteomalacia on the bone mineralization process. *Calcif Tissue Int*. 2009;84(4):313–23. <https://doi.org/10.1007/s00223-009-9216-z>.
55. Roschger P, Fratzl-Zelman N, Misof BM, Glorieux FH, Klaushofer K, Rauch F. Evidence that abnormal high bone mineralization in growing children with osteogenesis imperfecta is not associated with specific collagen mutations. *Calcif Tissue Int*. 2008;82(4):263–70. <https://doi.org/10.1007/s00223-008-9113-x>.
56. Buenzli PR, Lerebours C, Roschger A, Roschger P, Weinkamer R. Late stages of mineralization and their

- signature on the bone mineral density distribution. *Connect Tissue Res.* 2018;59(sup1):74–80. <https://doi.org/10.1080/03008207.2018.1424149>.
57. Lukas C, Ruffoni D, Lambers FM, Schulte FA, Kuhn G, Kollmannsberger P, Weinkamer R, Müller R. Mineralization kinetics in murine trabecular bone quantified by time-lapsed in vivo micro-computed tomography. *Bone.* 2013;56(1):55–60. <https://doi.org/10.1016/j.bone.2013.05.005>.
58. Kristensen E, Hallgrímsson B, Morck DW, Boyd SK. Timing of growth hormone treatment affects trabecular bone microarchitecture and mineralization in growth hormone deficient mice. *Bone.* 2010;47:295–300.
59. Akkus O, Polyakova-Akkus A, Adar F, Schaffler MB. Aging of microstructural compartments in human compact bone. *J Bone Miner Res.* 2003;18(6):1012–9.
60. Bala Y, Farlay D, Delmas PD, Meunier PJ, Boivin G. Time sequence of secondary mineralization and microhardness in cortical and cancellous bone from ewes. *Bone.* 2010;46(4):1204–12. <https://doi.org/10.1016/j.bone.2009.11.032>.
61. Fuchs RK, Allen MR, Ruppel ME, Diab T, Phipps RJ, Miller LM, Burr DB. In situ examination of the time-course for secondary mineralization of haversian bone using synchrotron Fourier transform infrared micro-spectroscopy. *Matrix Biol.* 2008;27(1):34–41.
62. Gamsjaeger S, Hofstetter B, Fratzl-Zelman N, Roschger P, Roschger A, Fratzl P, Brozek W, Masic A, Misof BM, Glorieux FH, Klaushofer K, Rauch F, Paschalis EP. Pediatric reference Raman data for material characteristics of iliac trabecular bone. *Bone.* 2014;69:89–97. <https://doi.org/10.1016/j.bone.2014.09.012>.
63. Roschger P, Paschalis EP, Fratzl P, Klaushofer K. Bone mineralization density distribution in health and disease. *Bone.* 2008;42(3):456–66. Epub 2007 Nov 12. Review.
64. Misof BM, Roschger P, Cosman R, Kurland ES, Tesch W, Messmer P, Dempster DW, Nieves J, Shane E, Fratzl P, Klaushofer K, Bilezikian J, Lindsay R. Effects of intermittent parathyroid hormone administration on bone mineralization density distribution in iliac crest biopsies from patients with osteoporosis: a paired study before and after treatment. *J Clin Endocrinol Metab.* 2003;88:1150–6.
65. Hasegawa T. Ultrastructure and biological function of matrix vesicles in bone mineralization. *Histochem Cell Biol.* 2018;149(4):289–304. <https://doi.org/10.1007/s00418-018-1646-0>. Review.
66. Skedros JG, Holmes JL, Vajda EG, Bloebaum RD. Cement lines of secondary osteons in human bone are not mineral-deficient: new data in a historical perspective. *Anat Rec A Discov Mol Cell Evol Biol.* 2005;286(1):781–803.
67. Milovanovic P, Vom Scheidt A, Mletzko K, Sarau G, Püschel K, Djuric M, Amling M, Christiansen S, Busse B. Bone tissue aging affects mineralization of cement lines. *Bone.* 2018;110:187–93. <https://doi.org/10.1016/j.bone.2018.02.004>. Epub 2018 Feb 7.
68. Nyssen-Behets C, Arnould V, Dhém A. Hypermineralized lamellae below the bone surface: a quantitative microradiographic study. *Bone.* 1994;15(6):685–9.
69. Repp F, Kollmannsberger P, Roschger A, Kerschnitzki M, Berzlanovich A, Gruber GM, Roschger P, Wagermaier W, Weinkamer R. Spatial heterogeneity in the canalicular density of the osteocyte network in human osteons. *Bone Rep.* 2017;6:101–8. <https://doi.org/10.1016/j.bonr.2017.03.001>. eCollection 2017 Jun.
70. Hesse B, Varga P, Langer M, Pacureanu A, Schrof S, Männicke N, Suhonen H, Maurer P, Cloetens P, Peyrin F, Raun K. Canalicular network morphology is the major determinant of the spatial distribution of mass density in human bone tissue: evidence by means of synchrotron radiation phase-contrast nano-CT. *J Bone Miner Res.* 2015;30(2):346–56. <https://doi.org/10.1002/jbmr.2324>.
71. Lees S. Considerations regarding the structure of the mammalian osteoid from viewpoint of the generalized packing model. *Connect Tissue Res.* 1987;16:281–303.
72. Boskey A, Camacho NP. FT-IR imaging of native and tissue-engineered bone and cartilage. *Biomaterials.* 2007;28:2465–78.
73. Paschalis EP, Gamsjaeger S, Fratzl-Zelman N, Roschger P, Masic A, Brozek W, Hassler N, Glorieux FH, Rauch F, Klaushofer K, Fratzl P. Evidence for a role for Nanoporosity and Pyridinoline content in human mild osteogenesis imperfecta. *J Bone Miner Res.* 2016;31(5):1050–9. <https://doi.org/10.1002/jbmr.2780>.
74. Jäger I, Fratzl P. Mineralized collagen fibrils: a mechanical model with a staggered arrangement of mineral particles. *Biophys J.* 2000;79(4):1737–46.
75. Roschger A, Gamsjaeger S, Hofstetter B, Masic A, Blouin S, Messmer P, Berzlanovich A, Paschalis EP, Roschger P, Klaushofer K, Fratzl P. Relationship between the $\nu_2\text{PO}_4/\text{amide III}$ ratio assessed by Raman spectroscopy and the calcium content measured by quantitative backscattered electron microscopy in healthy human osteonal bone. *J Biomed Opt.* 2014;19(6):065002. <https://doi.org/10.1117/1.JBO.19.6.065002>.
76. Masic A, Bertinetti L, Schuetz R, Chang SW, Metzger TH, Buehler MJ, Fratzl P. Osmotic pressure induced tensile forces in tendon collagen. *Nat Commun.* 2015;6:5942. <https://doi.org/10.1038/ncomms6942>.
77. Bertinetti L, Masic A, Schuetz R, Barbetta A, Seidt B, Wagermaier W, Fratzl P. Osmotically driven tensile stress in collagen-based mineralized tissues. *J Mech Behav Biomed Mater.* 2015;52:14–21. <https://doi.org/10.1016/j.jmbbm.2015.03.010>.
78. Roschger P, Grabner BM, Rinnerthaler S, Tesch W, Kneissel M, Berzlanovich A, Klaushofer K, Fratzl P. Structural development of the mineralized tissue in the human L4 vertebral body. *J Struct Biol.* 2001;136(2):126–36.

79. Fratzl-Zelman N, Schmidt I, Roschger P, Glorieux FH, Klaushofer K, Fratzl P, Rauch F, Wagermaier W. Mineral particle size in children with osteogenesis imperfecta type I is not increased independently of specific collagen mutations. *Bone*. 2014;60:122–8. <https://doi.org/10.1016/j.bone.2013.11.023>.
80. Fratzl-Zelman N, Misof BM, Klaushofer K, Roschger P. Bone mass and mineralization in osteogenesis imperfecta. *Wien Med Wochenschr*. 2015;165(13–14):271–7. <https://doi.org/10.1007/s10354-015-0369-2>. Epub 2015 Jul 25. Review.
81. Boyde A, Travers R, Glorieux FH, Jones SJ. The mineralization density of iliac crest bone from children with osteogenesis imperfecta. *Calcif Tissue Int*. 1999;64(3):185–90.
82. Jones SJ, Glorieux FH, Travers R, Boyde A. The microscopic structure of bone in normal children and patients with osteogenesis imperfecta: a survey using backscattered electron imaging. *Calcif Tissue Int*. 1999;64(1):8–17.
83. Granke M, Does MD, Nyman JS. The role of water compartments in the material properties of cortical bone. *Calcif Tissue Int*. 2015;97(3):292–307. <https://doi.org/10.1007/s00223-015-9977-5>. Review.
84. Wang X, Xu H, Huang Y, Gu S, Jiang JX. Coupling effect of water and proteoglycans on the in situ toughness of bone. *J Bone Miner Res*. 2016;31(5):1026–9. <https://doi.org/10.1002/jbmr.2774>.
85. Ruffoni D, Fratzl P, Roschger P, Klaushofer K, Weinkamer R. The bone mineralization density distribution as a fingerprint of the mineralization process. *Bone*. 2007;40(5):1308–19.
86. Grynopas M. Age and disease-related changes in the mineral of bone. *Calcif Tissue Int*. 1993;53(Suppl1):S57–64.
87. Fratzl-Zelman N, Roschger P, Misof BM, Pfeffer S, Glorieux FH, Klaushofer K, Rauch F. Normative data on mineralization density distribution in iliac bone biopsies of children, adolescents and young adults. *Bone*. 2009;44(6):1043–8. <https://doi.org/10.1016/j.bone.2009.02.021>.
88. Boivin G, Meunier PJ. Changes in bone remodeling rate influence the degree of mineralization of bone. *Connect Tissue Res*. 2002;43(2–3):535–7.
89. Fratzl P, Roschger P, Fratzl-Zelman N, Paschalis EP, Phipps R, Klaushofer K. Evidence that treatment with risedronate in women with postmenopausal osteoporosis affects bone mineralization and bone volume. *Calcif Tissue Int*. 2007;81(2):73–80.
90. Carden A, Morris MD. Application of vibrational spectroscopy to the study of mineralized tissues (review). *J Biomed Opt*. 2000;5(3):259–68. Review.
91. Boskey AL. Assessment of bone mineral and matrix using backscatter electron imaging and FTIR imaging. *Curr Osteoporos Rep*. 2006;4(2):71–5. Review.
92. Gamsjaeger S, Mendelsohn R, Boskey AL, Gourion-Arsiquaud S, Klaushofer K, Paschalis EP. Vibrational spectroscopic imaging for the evaluation of matrix and mineral chemistry. *Curr Osteoporos Rep*. 2014;12(4):454–64. <https://doi.org/10.1007/s11914-014-0238-8>. Review.
93. Paschalis EP, Gamsjaeger S, Klaushofer K. Vibrational spectroscopic techniques to assess bone quality. *Osteoporos Int*. 2017;28(8):2275–91. <https://doi.org/10.1007/s00198-017-4019-y>. Review.
94. Kovarik J, Willvonseder R, Plenk H Jr, Böhler N, Woloszczuk W, Eschberger J, Dorda W, Haber P. Evidence for negative correlation between quantitative histological studies and microradiography of iliac crest bone and forearm osteodensitometry in elderly women with osteoporosis. *Calcif Tissue Int*. 1982;34(5):456–8.
95. Boivin G, Meunier PJ. The degree of mineralization of bone tissue measured by computerized quantitative contact microradiography. *Calcif Tissue Int*. 2002;70:503–11.
96. Montagner F, Kaftandjian V, Farlay D, Brau D, Boivin G, Follet H. Validation of a novel microradiography device for characterization of bone mineralization. *J Xray Sci Technol*. 2015;23(2):201–11. <https://doi.org/10.3233/XST-150481>.
97. Nuzzo S, Lafage-Proust MH, Martin-Badosa E, Boivin G, Thomas T, Alexandre C, Peyrin F. Synchrotron radiation microtomography allows the analysis of three-dimensional microarchitecture and degree of mineralization of human iliac crest biopsy specimens: effect of etidronate treatment. *J Bone Miner Res*. 2002;17:1372–82.
98. Borah B, Ritman EL, Dufresne TE, Jorgensen SM, Liu S, Sacha J, Phipps RJ, Turner RT. The effect of risedronate on bone mineralization as measured by micro-computed tomography with synchrotron radiation: correlation to histomorphometric indices of turnover. *Bone*. 2005;37:1–9.
99. Bortel EL, Langer M, Rack A, Forien J-B, Duda GN, Fratzl P, Zaslansky P. Combining coherent hard X-ray tomographies with phase retrieval to generate three-dimensional models of forming bone. *Front Mater*. 2017;4:39.
100. Boyde A, Jones SJ. Backscattered electron imaging of skeletal tissues. *Metab Bone Dis Rel Res*. 1983;5:145–50.
101. Bloebaum RD, Skedros JG, Vajda EG, Bachus KN, Constantz BR. Determining mineral content variations in bone using backscattered electron imaging. *Bone*. 1997;20:485–90.
102. Roschger P, Fratzl P, Eschberger J, Klaushofer K. Validation of quantitative backscattered electron imaging for the measurement of mineral density distribution in human bone biopsies. *Bone*. 1998;23:319–26.
103. Roschger P, Gupta HS, Berzlanovich A, Ittner G, Dempster DW, Fratzl P, Cosman F, Parisien M, Lindsay R, Nieves JW, Klaushofer K. Constant mineralization density distribution in cancellous human bone. *Bone*. 2003;32:316–23.
104. Koehne T, Vettorazzi E, Küsters N, Lüneburg R, Kahl-Nieke B, Püschel K, Amling M, Busse B. Trends in trabecular architecture and bone mineral density distribution in 152 individuals aged

- 30–90 years. *Bone*. 2014;66:31–8. <https://doi.org/10.1016/j.bone.2014.05.010>.
105. Misof BM, Gamsjaeger S, Cohen A, Hofstetter B, Roschger P, Stein E, Nickolas TL, Rogers HF, Dempster D, Zhou H, Recker R, Lappe J, McMahon D, Paschalis EP, Fratzl P, Shane E, Klaushofer K. Bone material properties in premenopausal women with idiopathic osteoporosis. *J Bone Miner Res*. 2012;27(12):2551–61. <https://doi.org/10.1002/jbmr.1699>.
 106. Balasubramanian M, Fratzl-Zelman N, O'Sullivan R, Bull M, Fa Peel N, Pollitt RC, Jones R, Milne E, Smith K, Roschger P, Klaushofer K, Bishop NJ. Novel PLS3 variants in X-linked osteoporosis: exploring bone material properties. *Am J Med Genet A*. 2018; <https://doi.org/10.1002/ajmg.a.38830>. [Epub ahead of print].
 107. Blouin S, Fratzl-Zelman N, Glorieux FH, Roschger P, Klaushofer K, Marini JC, Rauch F. Hypermineralization and high osteocyte lacunar density in osteogenesis imperfecta type V bone indicate exuberant primary bone formation. *J Bone Miner Res*. 2017;32(9):1884–92. <https://doi.org/10.1002/jbmr.3180>. Epub 2017 Jun 26.
 108. Webb EA, Balasubramanian M, Fratzl-Zelman N, Cabral WA, Titheradge H, Alsaedi A, Saraff V, Vogt J, Cole T, Stewart A, Crabtree NJ, Sargent BM, Gamsjaeger S, Paschalis EP, Roschger P, Klaushofer K, Shaw NJ, Marini JC, Högler W. Phenotypic Spectrum in osteogenesis imperfecta due to mutations in TMEM38B: unravelling a complex cellular defect. *J Clin Endocrinol Metab*. 2017;102(6):2019–28. <https://doi.org/10.1210/jc.2016-3766>.
 109. Ciarelli TE, Fyhrie DP, Parfitt AM effects of vertebral bone fragility and bone formation rate on the mineralization levels of cancellous bone from white females. *Bone*. 2003;32(3):311–5.
 110. Fratzl P. Bone fracture: when the cracks begin to show. *Nat Mater*. 2008;7(8):610–2.
 111. Koester KJ, Ager JW 3rd, Ritchie RO. The true toughness of human cortical bone measured with realistically short cracks. *Nat Mater*. 2008;7(8):672–7.
 112. Donnelly E, Meredith DS, Nguyen JT, Boskey AL. Bone tissue composition varies across anatomic sites in the proximal femur and the iliac crest. *J Orthop Res*. 2012;30(5):700–6. <https://doi.org/10.1002/jor.21574>.
 113. Kingsmill VJ, Gray CM, Moles DR, Boyde A. Cortical vascular canals in human mandible and other bones. *J Dent Res*. 2007;86(4):368–72.
 114. Fratzl-Zelman N, Roschger P, Gourrier A, Weber M, Misof BM, Loveridge N, Reeve J, Klaushofer K, Fratzl P. Combination of nanoindentation and quantitative backscattered electron imaging revealed altered bone material properties associated with femoral neck fragility. *Calcif Tissue Int*. 2009;85(4):335–43. <https://doi.org/10.1007/s00223-009-9289-8>.
 115. Loveridge N, Power J, Reeve J, Boyde A. Bone mineralization density and femoral neck fragility. *Bone*. 2004;35(4):929–41.
 116. Parfitt AM. Misconceptions (2): turnover is always higher in cancellous than in cortical bone. *Bone*. 2002;30:807–9.
 117. Duboeuf F, Burt-Pichat B, Farlay D, Suy P, Truy E, Boivin G. Bone quality and biomechanical function: a lesson from human ossicles. *Bone*. 2015;73:105–10. <https://doi.org/10.1016/j.bone.2014.12.009>.
 118. Misof BM, Dempster DW, Zhou H, Roschger P, Fratzl-Zelman N, Fratzl P, Silverberg SJ, Shane E, Cohen A, Stein E, Nickolas TL, Recker RR, Lappe J, Bilezikian JP, Klaushofer K. Relationship of bone mineralization density distribution (BMDD) in cortical and cancellous bone within the iliac crest of healthy premenopausal women. *Calcif Tissue Int*. 2014;95(4):332–9. <https://doi.org/10.1007/s00223-014-9901-4>.
 119. Eastell R, O'Neill TW, Hofbauer LC, Langdahl B, Reid IR, Gold DT, Cummings SR. Postmenopausal osteoporosis. *Nat Rev Dis Primers*. 2016;2:16069. <https://doi.org/10.1038/nrdp.2016.69>. Review.
 120. Whyte MP, Bergfeld MA, Murphy WA, Avioli LV, Teitelbaum SL. Postmenopausal osteoporosis: a heterogeneous disorder as assessed by histomorphometric analysis of iliac crest bone from untreated patients. *Am J Med*. 1982;72:193–202.
 121. Arlot ME, Delmas PD, Cappard D, Meunier PJ. Trabecular and endocortical bone remodeling in postmenopausal osteoporosis: comparison with normal postmenopausal women. *Osteoporosis Int*. 1990;1:41–9.
 122. Rehman MTA, Hoyland JA, Denton J, Freemont AJ. Histomorphometric classification of postmenopausal osteoporosis: implications for the management of osteoporosis. *J Clin Pathol*. 1995;48:229–35.
 123. Recker R, Lappe J, Davies KM, Heaney R. Bone remodeling increases substantially in the years after menopause and remains increased in older osteoporosis patients. *J Bone Miner Res*. 2004;19:1628–33.
 124. Han Z-H, Palnitkar S, Sudhaker Rao D, Nelson D, Parfitt AM. Effects of ethnicity and age or menopause on the remodeling and turnover of iliac bone: implications for mechanisms of bone loss. *J Bone Miner Res*. 1997;12:498–508.
 125. Borah B, Dufresne TE, Ritman EL, Jorgensen SM, Liu S, Chmielewski PA, Phipps RJ, Zhou X, Sibonga JD, Turner RT. Long-term risedronate treatment normalizes mineralization and continues to preserve trabecular architecture: sequential triple biopsy studies with micro-computed tomography. *Bone*. 2006;39:345–52.
 126. Roschger P, Rinnerthaler S, Yates J, Rodan GA, Fratzl P, Klaushofer K. Alendronate increases degree and uniformity of mineralization in cancellous bone and decreases the porosity in cortical bone of osteoporotic women. *Bone*. 2001;29(2):185–91.
 127. Faibish D, Ott SM, Boskey AL. Mineral changes in osteoporosis. *A Review Clin Orthop Relat Res*. 2006;443:28–38.

128. Zoehrer R, Roschger P, Fratzl P, Durchschlag E, Paschalis E, Phipps R, Klaushofer K. Effects of 3- and 5-year treatment with risedronate on the bone mineral density distribution of cancellous bone in human iliac crest biopsies. *J Bone Miner Res.* 2006;21:1106–12.
129. Boskey AL, DiCarlo E, Paschalis E, West P, Mendelsohn R. Comparison of mineral quality and quantity in iliac crest biopsies from high- and low-turnover osteoporosis: an FT-IR microspectroscopic investigation. *Osteoporos Int.* 2005;16(12):2031–8.
130. Roschger P, Misof B, Paschalis E, Fratzl P, Klaushofer K. Changes in the degree of mineralization with osteoporosis and its treatment. *Curr Osteoporos Rep.* 2014;12(3):338–50. <https://doi.org/10.1007/s11914-014-0218-z>. Review.
131. Dempster DW, Brown JP, Fahrleitner-Pammer A, Kendler D, Rizzo S, Valter I, Wagman RB, Yin X, Yue SV, Boivin G. Effects of long-term denosumab on bone histomorphometry and mineralization in women with postmenopausal osteoporosis. *J Clin Endocrinol Metab.* 2018; <https://doi.org/10.1210/jc.2017-02669>. [Epub ahead of print].
132. Roschger P, Dempster DW, Zhou H, Paschalis EP, Silverberg SJ, Shane E, Bilezikian JP, Klaushofer K. New observations on bone quality in mild primary hyperparathyroidism as determined by quantitative backscattered electron imaging. *J Bone Miner Res.* 2007;22:717–23.
133. Misof BM, Roschger P, Dempster DW, Zhou H, Bilezikian JP, Klaushofer K, Rubin MR. PTH(1-84) administration in hypoparathyroidism transiently reduces bone matrix mineralization. *J Bone Miner Res.* 2016;31(1):180–9. <https://doi.org/10.1002/jbmr.2588>.
134. Misof BM, Roschger P, Klaushofer K, Rauch F, Ma J, Mack DR, Ward LM. Increased bone matrix mineralization in treatment-naïve children with inflammatory bowel disease. *Bone.* 2017;105:50–6. <https://doi.org/10.1016/j.bone.2017.07.011>.
135. Fratzl-Zelman N, Valta H, Pereira RC, Misof BM, Roschger P, Jalanko H, Wesseling-Perry K, Klaushofer K, Mäkitie O. Abnormally high and heterogeneous bone matrix mineralization after childhood solid organ transplantation: a complex pathology of low bone turnover and local defects in mineralization. *J Bone Miner Res.* 2017;32(5):1116–25. <https://doi.org/10.1002/jbmr.3087>.
136. Nawrot-Wawrzyniak K, Misof BM, Roschger P, Pańczyk-Tomaszewska M, Ziółkowska H, Klaushofer K, Fratzl-Zelman N changes in bone matrix mineralization after growth hormone treatment in children and adolescents with chronic kidney failure treated by dialysis: a paired biopsy study. *Am J Kidney Dis.* 2013;61(5):767–77.
137. Gourion-Arsiquaud S, Lukashova L, Power J, Loveridge N, Reeve J, Boskey AL. Fourier transform infrared imaging of femoral neck bone: reduced heterogeneity of mineral-to-matrix and carbonate-to-phosphate and more variable crystallinity in treatment-naïve fracture cases compared with fracture-free controls. *J Bone Miner Res.* 2013;28(1):150–61. <https://doi.org/10.1002/jbmr.1724>.
138. Paschalis EP, Gamsjaeger S, Dempster D, Jorgetti V, Borba V, Boguszewski CL, Klaushofer K, Moreira CA. Fragility fracture incidence in chronic obstructive pulmonary disease (COPD) patients associates with Nanoporosity, mineral/matrix ratio, and Pyridinoline content at actively bone-forming trabecular surfaces. *J Bone Miner Res.* 2017;32(1):165–71. <https://doi.org/10.1002/jbmr.2933>.
139. Seitz S, Koehne T, Ries C, De Novo OA, Barvencik F, Busse B, Eulenburger C, Schinke T, Püschel K, Rueger JM, Amling M, Pogoda P. Impaired bone mineralization accompanied by low vitamin D and secondary hyperparathyroidism in patients with femoral neck fracture. *Osteoporos Int.* 2013;24(2):641–9. <https://doi.org/10.1007/s00198-012-2011-0>.
140. Boivin G, Bala Y, Doublier A, Farlay D, Ste-Marie LG, Meunier PJ, Delmas PD. The role of mineralization and organic matrix in the microhardness of bone tissue from controls and osteoporotic patients. *Bone.* 2008;43:532–8.
141. Fratzl-Zelman N, Roschger P, Misof BM, Nawrot-Wawrzyniak K, Pötter-Lang S, Muschitz C, Resch H, Klaushofer K, Zwettler E. Fragility fractures in men with idiopathic osteoporosis are associated with undermineralization of the bone matrix without evidence of increased bone turnover. *Calcif Tissue Int.* 2011;88(5):378–87.
142. Misof BM, Patsch JM, Roschger P, Muschitz C, Gamsjaeger S, Paschalis EP, Prokop E, Klaushofer K, Pietschmann P, Resch H. Intravenous treatment with ibandronate normalizes bone matrix mineralization and reduces cortical porosity after two years in male osteoporosis: a paired biopsy study. *J Bone Miner Res.* 2013; <https://doi.org/10.1002/jbmr.2035>.
143. Stewart TL, Roschger P, Misof BM, Mann V, Fratzl P, Klaushofer K, Aspden R, Ralston SH association of COLIA1 Sp1 alleles with defective bone nodule formation in vitro and abnormal bone mineralization in vivo. *Calcif Tissue Int.* 2005;77(2):113–8.
144. Braga V, Gatti D, Rossini M, Colapietro F, Battaglia E, Viapiana O, Adami S. Bone turnover markers in patients with osteogenesis imperfecta. *Bone.* 2004;34(6):1013–6.
145. Bishop N. Bone material properties in osteogenesis imperfecta. *J Bone Miner Res.* 2016;31(4):699–708. <https://doi.org/10.1002/jbmr.2835>. Review.
146. Lindahl K, Barnes AM, Fratzl-Zelman N, Whyte MP, Hefferan TE, Makareeva E, Brusel M, Yaszemski MJ, Rubin CJ, Kindmark A, Roschger P, Klaushofer K, McAlister WH, Mumm S, Leikin S, Kessler E, Boskey AL, Ljunggren O, Marini JC. COL1 C-propeptide cleavage site mutations cause high bone mass osteogenesis imperfecta. *Hum Mutat.* 2011;32(6):598–609. <https://doi.org/10.1002/humu.21475>.

147. Cundy T, Dray M, Delahunt J, Hald JD, Langdahl B, Li C, Szybowska M, Mohammed S, Duncan EL, McInerney-Leo AM, Wheeler PG, Roschger P, Klaushofer K, Rai J, Weis M, Eyre D, Schwarze U, Byers PH. Mutations that Alter the carboxy-terminal-Propeptide cleavage site of the chains of type I procollagen are associated with a unique osteogenesis imperfecta phenotype. *J Bone Miner Res.* 2018; <https://doi.org/10.1002/jbmr.3424>. [Epub ahead of print].
148. Fratzl-Zelman N, Schmidt I, Roschger P, Roschger A, Glorieux FH, Klaushofer K, Wagermaier W, Rauch F, Fratzl P. Unique micro- and nano-scale mineralization pattern of human osteogenesis imperfecta type VI bone. *Bone.* 2015;73:233–41. <https://doi.org/10.1016/j.bone.2014.12.023>.
149. Cheung M, Roschger P, Klaushofer K, Veilleux LN, Roughley P, Glorieux FH, Rauch F. Cortical and trabecular bone density in X-linked hypophosphatemic rickets. *J Clin Endocrinol Metab.* 2013;98(5):E954–61. <https://doi.org/10.1210/jc.2012-4133>. Epub 2013 Mar 26.
150. Bartko J, Roschger P, Zandieh S, Brehm A, Zwerina J, Klaushofer K. Hypophosphatemia, severe bone pain, gait disturbance, and fatigue fractures after Iron substitution in inflammatory bowel disease: a case report. *J Bone Miner Res.* 2018;33(3):534–9. <https://doi.org/10.1002/jbmr.3319>.
151. Whyte MP. Hypophosphatasia – aetiology, nosology, pathogenesis, diagnosis and treatment. *Nat Rev Endocrinol.* 2016;12(4):233–46. <https://doi.org/10.1038/nrendo.2016.14>. Review.
152. Whyte MP, Rockman-Greenberg C, Ozono K, Riese R, Moseley S, Melian A, Thompson DD, Bishop N, Hofmann C. Asfotase alfa treatment improves survival for perinatal and infantile hypophosphatasia. *J Clin Endocrinol Metab.* 2016;101(1):334–42. <https://doi.org/10.1210/jc.2015-3462>.
153. Mornet E. Hypophosphatasia. *Metabolism.* 2018;82:142–55. <https://doi.org/10.1016/j.metabol.2017.08.013>. Epub 2017 Sep 20. Review.
154. Berkseth KE, Tebben PJ, Drake MT, Hefferan TE, Jewison DE, Wermers RA. Clinical spectrum of hypophosphatasia diagnosed in adults. *Bone.* 2013;54(1):21–7. <https://doi.org/10.1016/j.bone.2013.01.024>.
155. Barvencik F, Beil FT, Gebauer M, Busse B, Koehne T, Seitz S, Zustin J, Pogoda P, Schinke T, Amling M. Skeletal mineralization defects in adult hypophosphatasia – a clinical and histological analysis. *Osteoporos Int.* 2011;22(10):2667–75. <https://doi.org/10.1007/s00198-011-1528-y>.
156. Whyte MP. Hypophosphatasia: enzyme replacement therapy brings new opportunities and new challenges. *J Bone Miner Res.* 2017;32(4):667–75. <https://doi.org/10.1002/jbmr.3075>. Review.
157. Liu J, Campbell C, Nam HK, Caron A, Yadav MC, Millán JL, Hatch NE. Enzyme replacement for craniofacial skeletal defects and craniosynostosis in murine hypophosphatasia. *Bone.* 2015;78:203–11. <https://doi.org/10.1016/j.bone.2015.05.005>.
158. Gasque KC, Foster BL, Kuss P, Yadav MC, Liu J, Kiffer-Moreira T, van Elsland A, Hatch N, Somerman MJ, Millán JL. Improvement of the skeletal and dental hypophosphatasia phenotype in *Alpl*^{-/-} mice by administration of soluble (non-targeted) chimeric alkaline phosphatase. *Bone.* 2015;72:137–47. <https://doi.org/10.1016/j.bone.2014.11.017>.
159. Dempster DW, Roschger P, Misof BM, Zhou H, Paschalis EP, Alam J, Ruff VA, Klaushofer K, Taylor KA. Differential effects of teriparatide and zoledronic acid on bone mineralization density distribution at 6 and 24 months in the SHOTZ study. *J Bone Miner Res.* 2016;31(8):1527–35. <https://doi.org/10.1002/jbmr.2825>.
160. Naylor KE, Jacques RM, Paggiosi M, Gossiel F, Peel NF, McCloskey EV, Walsh JS, Eastell R. Response of bone turnover markers to three oral bisphosphonate therapies in postmenopausal osteoporosis: the TRIO study. *Osteoporos Int.* 2016;27(1):21–31. <https://doi.org/10.1007/s00198-015-3145-7>.
161. Ruffoni D, Fratzl P, Roschger P, Phipps R, Klaushofer K, Weinkamer R. Effect of temporal changes in bone turnover on the bone mineralization density distribution: a computer simulation study. *J Bone Miner Res.* 2008;23(12):1905–14. <https://doi.org/10.1359/jbmr.080711>.
162. Boivin G, Lips P, Ott SM, Harper KD, Sarkar S, Pinette KV, Meunier PJ. Contribution of raloxifene and calcium and vitamin D3 supplementation to the increase of the degree of mineralization of bone in postmenopausal women. *J Clin Endocrinol Metab.* 2003;88(9):4199–205.
163. McClung MR. New management options for osteoporosis with emphasis on SERMs. *Climacteric.* 2015;18(Suppl 2):56–61. <https://doi.org/10.3109/13697137.2015.1104010>. Review.
164. Boivin G, Vedi S, Purdie DW, Compston JE, Meunier PJ. Influence of estrogen therapy at conventional and high doses on the degree of mineralization of iliac bone tissue: a quantitative microradiographic analysis in postmenopausal women. *Bone.* 2005;36:562–7.
165. Paschalis EP, Boskey AL, Kassem M, Eriksen EF. Effect of hormone replacement therapy on bone quality in early postmenopausal women. *J Bone Miner Res.* 2003;18(6):955–9.
166. Russell RG. Bisphosphonates: the first 40 years. *Bone.* 2011;49(1):2–19. <https://doi.org/10.1016/j.bone.2011.04.022>. Review.
167. Kenkre JS, Bassett J. The bone remodelling cycle. *Ann Clin Biochem.* 2018;55(3):308–27. <https://doi.org/10.1177/0004563218759371>. Epub 2018 Mar 4.
168. Roschger P, Lombardi A, Misof BM, Maier G, Fratzl-Zelman N, Kimmel D, LaMotta A, Fratzl P, Klaushofer K. Mineralization density distribution of postmenopausal osteoporotic bone is restored to normal after long-term alendronate treatment: qBEI and sSAXS data from the fracture intervention trial

- long-term extension (FLEX). *J Bone Miner Res.* 2010;25:48–55.
169. Shane E, Burr D, Abrahamson B, Adler RA, Brown TD, Cheung AM, Cosman F, Curtis JR, Dell R, Dempster DW, Ebeling PR, Einhorn TA, Genant HK, Geusens P, Klaushofer K, Lane JM, McKiernan F, McKinney R, Ng A, Nieves J, O'Keefe R, Papapoulos S, Howe TS, van der Meulen MC, Weinstein RS, Whyte MP. Atypical subtrochanteric and diaphyseal femoral fractures: second report of a task force of the American society for bone and mineral research. *J Bone Miner Res.* 2014;29(1):1–23. <https://doi.org/10.1002/jbmr.1998>.
 170. Misof BM, Roschger P, Gabriel D, Paschalis EP, Eriksen EF, Recker RR, Gasser JA, Klaushofer K. Annual intravenous zoledronic acid for three years increased cancellous bone matrix mineralization beyond normal values in the HORIZON biopsy cohort. *J Bone Miner Res.* 2013;28(3):442–8. <https://doi.org/10.1002/jbmr.1780>.
 171. Krause M, Soltan M, Zimmermann EA, Hahn M, Kornet J, Hapfelmeier A, Breer S, Morlock M, Wulff B, Püschel K, Glueer CC, Amling M, Busse B. Effects of long-term alendronate treatment on bone mineralisation, resorption parameters and biomechanics of single human vertebral trabeculae. *Eur Cell Mater.* 2014;28:152–63; discussion 163–5.
 172. Misof BM, Roschger P, McMillan HJ, Ma J, Klaushofer K, Rauch F, Ward LM. Histomorphometry and bone matrix mineralization before and after bisphosphonate treatment in boys with Duchenne muscular dystrophy: a paired Transiliac biopsy study. *J Bone Miner Res.* 2016;31(5):1060–9. <https://doi.org/10.1002/jbmr.2756>.
 173. Misof BM, Blouin S, Lueger S, Paschalis EP, Recker RR, Phipps R, Klaushofer K, Roschger P. Baseline mineralizing surface determines the magnitude of the bisphosphonate effect on cortical bone mineralization in postmenopausal osteoporotic patients. *J Musculoskelet Neuronal Interact.* 2017;17(3):183–91.
 174. Fuchs RK, Faillace ME, Allen MR, Phipps RJ, Miller LM, Burr DB. Bisphosphonates do not alter the rate of secondary mineralization. *Bone.* 2011;49(4):701–5. <https://doi.org/10.1016/j.bone.2011.05.009>.
 175. Nancollas GH, Tang R, Phipps RJ, Henneman Z, Gulde S, Wu W, Mangood A, Russell RG, Ebetino FH. Novel insights into actions of bisphosphonates on bone: differences in interactions with hydroxyapatite. *Bone.* 2006;38(5):617–27.
 176. Hofstetter B, Gamsjaeger S, Phipps RJ, Recker RR, Ebetino FH, Klaushofer K, Paschalis EP. Effects of alendronate and risedronate on bone material properties in actively forming trabecular bone surfaces. *J Bone Miner Res.* 2012;27(5):995–1003. <https://doi.org/10.1002/jbmr.1572>.
 177. Gamsjaeger S, Buchinger B, Zoehrer R, Phipps R, Klaushofer K, Paschalis EP. Effects of one year daily teriparatide treatment on trabecular bone material properties in postmenopausal osteoporotic women previously treated with alendronate or risedronate. *Bone.* 2011;49(6):1160–5. <https://doi.org/10.1016/j.bone.2011.08.015>.
 178. Hofstetter B, Gamsjaeger S, Varga F, Dobnig H, Stepan JJ, Petto H, Pavo I, Klaushofer K, Paschalis EP. Bone quality of the newest bone formed after two years of teriparatide therapy in patients who were previously treatment-naïve or on long-term alendronate therapy. *Osteoporos Int.* 2014;25(12):2709–19. <https://doi.org/10.1007/s00198-014-2814-2>.
 179. Bone HG, Wagman RB, Brandi ML, Brown JP, Chapurlat R, Cummings SR, Czerwinski E, Fahrleitner-Pammer A, Kendler DL, Lippuner K, Reginster JY, Roux C, Malouf J, Bradley MN, Daizadeh NS, Wang A, Dakin P, Pannacciulli N, Dempster DW, Papapoulos S. 10 years of denosumab treatment in postmenopausal women with osteoporosis: results from the phase 3 randomised FREEDOM trial and open-label extension. *Lancet Diabetes Endocrinol.* 2017;5(7):513–23. [https://doi.org/10.1016/S2213-8587\(17\)30138-9](https://doi.org/10.1016/S2213-8587(17)30138-9).
 180. Reid IR, Miller PD, Brown JP, Kendler DL, Fahrleitner-Pammer A, Valter I, Maasalu K, Bolognese MA, Woodson G, Bone H, Ding B, Wagman RB, San Martin J, Ominsky MS, Dempster DW. Denosumab phase 3 bone histology study group. Effects of denosumab on bone histomorphometry: the FREEDOM and STAND studies. *J Bone Miner Res.* 2010;25(10):2256–65. <https://doi.org/10.1002/jbmr.149>.
 181. Marie PJ, Felsenberg D, Brandi ML. How strontium ranelate, via opposite effects on bone resorption and formation, prevents osteoporosis. *Osteoporos Int.* 2011;22(6):1659–67. <https://doi.org/10.1007/s00198-010-1369-0>. Review.
 182. Chavassieux P, Meunier PJ, Roux JP, Portero-Muzy N, Pierre M, Chapurlat R. Bone histomorphometry of transiliac paired bone biopsies after 6 or 12 months of treatment with oral strontium ranelate in 387 osteoporotic women. Randomized comparison to alendronate. *J Bone Miner Res.* 2013; <https://doi.org/10.1002/jbmr.2074>.
 183. Roschger P, Manjubala I, Zoeger N, Meirer F, Simon R, Li C, Fratzl-Zelman N, Misof BM, Paschalis EP, Strelci C, Fratzl P, Klaushofer K. Bone material quality in transiliac bone biopsies of postmenopausal osteoporotic women after 3 years of strontium ranelate treatment. *J Bone Miner Res.* 2010;25(4):891–900. <https://doi.org/10.1359/jbmr.091028>.
 184. Li C, Paris O, Siegel P, Roschger P, Paschalis EP, Klaushofer K, Fratzl P. Strontium is incorporated into mineral crystals only in newly formed bone during strontium ranelate treatment. *J Bone Miner Res.* 2010;25(5):968–75. <https://doi.org/10.1359/jbmr.091038>.
 185. Riedel C, Zimmermann EA, Zustin J, Niecke M, Amling M, Grynblas M, Busse B. The incorporation of fluoride and strontium in hydroxyapatite affects

- the composition, structure, and mechanical properties of human cortical bone. *J Biomed Mater Res A*. 2017;105(2):433–42. <https://doi.org/10.1002/jbm.a.35917>.
186. Riggs BL, Hodgson SF, O'Fallon WM, Chao EY, Wahner HW, Muhs JM, Cedel SL, Melton LJ 3rd. Effect of fluoride treatment on the fracture rate in postmenopausal women with osteoporosis. *N Engl J Med*. 1990;322(12):802–9.
187. Chachra D, Vieira AP, Grynblas MD. Fluoride and mineralized tissues. *Crit Rev Biomed Eng*. 2008;36(2–3):183–223. Review.
188. Fratzl P, Roschger P, Eschberger J, Abendroth B, Klaushofer K. Abnormal bone mineralization after fluoride treatment in osteoporosis: a small-angle x-ray-scattering study. *J Bone Miner Res*. 1994;9(10):1541–9.
189. Gourrier A, Li C, Seigel S, Paris O, Roschger P, Klaushofer K, Fratzl P. Scanning small-angle X-ray scattering analysis of the size and organization of the mineral nanoparticles in fluorotic bone using a stack of cards model. *J Appl Crystallogr*. 2010;43:1385–92.
190. Boivin G, Duriez J, Chapuy MC, Flautre B, Hardouin P, Meunier PJ. Relationship between bone fluoride content and histological evidence of calcification defects in osteoporotic women treated long term with sodium fluoride. *Osteoporos Int*. 1993;3(4):204–8.
191. Rubin CD, Pak CY, Adams-Huet B, Genant HK, Li J, Rao DS. Sustained-release sodium fluoride in the treatment of the elderly with established osteoporosis. *Arch Intern Med*. 2001;161(19):2325–33.
192. Paschalis EP, Glass EV, Donley DW, Eriksen EF. Bone mineral and collagen quality in iliac crest biopsies of patients given teriparatide: new results from the fracture prevention trial. *J Clin Endocrinol Metab*. 2005;90:4644–9.
193. Misof BM, Paschalis EP, Blouin S, Fratzl-Zelman N, Klaushofer K, Roschger P. Effects of 1 year of daily teriparatide treatment on iliacal bone mineralization density distribution (BMDD) in postmenopausal osteoporotic women previously treated with alendronate or risedronate. *J Bone Miner Res*. 2010;25(11):2297–303. <https://doi.org/10.1002/jbmr.198>.
194. Augustine M, Horwitz MJ. Parathyroid hormone and parathyroid hormone-related protein analogs as therapies for osteoporosis. *Curr Osteoporos Rep*. 2013;11(4):400–6.
195. Moreira CA, Fitzpatrick LA, Wang Y, Recker RR. Effects of abaloparatide-SC (BA058) on bone histology and histomorphometry: The ACTIVE phase 3 trial. *Bone*. 2017;97:314–9. <https://doi.org/10.1016/j.bone.2016.11.004>.
196. Ross RD, Edwards LH, Acerbo AS, Ominsky MS, Virdi AS, Sena K, Miller LM, Sumner DR. Bone matrix quality after sclerostin antibody treatment. *J Bone Miner Res*. 2014;29(7):1597–607. <https://doi.org/10.1002/jbmr.2188>.
197. Roschger A, Roschger P, Keplingter P, Klaushofer K, Abdullah S, Kneissel M, Rauch F. Effect of sclerostin antibody treatment in a mouse model of severe osteogenesis imperfecta. *Bone*. 2014;66:182–8. <https://doi.org/10.1016/j.bone.2014.06.015>.